INVITED PAPER

Characterization of Human Motor Units From Surface EMG Decomposition

The study of motor units provides a window into the mechanisms of neural control of movement in humans. This paper reviews processing methods of the surface EMG signal to reliably characterize individual motor units in vivo in humans.

By Dario Farina, *Senior Member IEEE*, and Aleš Holobar, *Member IEEE*

ABSTRACT | Motor units are the smallest functional units of our movements. The study of their activation provides a window into the mechanisms of neural control of movement in humans. The classic methods for motor unit investigations date to several decades ago. They are based on invasive recordings with selective needle or wire electrodes. Conversely, the noninvasive (surface) EMG has been commonly processed as an interference signal, with the extraction of its global characteristics, e.g., amplitude. These characteristics, however, are only crudely associated to the underlying motor unit activities. In the last decade, methods have been proposed for reliably extracting individual motor unit activities from the interference surface EMG signal. We describe these methods in this review, with a focus on blind source separation (BSS) and techniques used on decomposed EMG signals. For example, from the motor unit discharge timings, information can be extracted regarding the synaptic input received by the corresponding motor neurons. In reviewing these methods, we also provide examples of applications in representative conditions, such as pathological tremor. In conclusion, we provide an overview of processing methods of the surface EMG signal that allow a reliable characterization of individual motor units *in vivo* in humans.

KEYWORDS | Blind source separation (BSS); decomposition; delay estimators; EMG; motor neuron; motor unit; spatial filters

I. INTRODUCTION

Surface electromyogram (EMG) has been classically considered as an electrophysiological technique to infer the global level of muscle activation [16], [28]. The information extracted from the surface EMG in most applications is indeed associated to the signal amplitude or power [28]. For example, surface EMG is commonly used to extract the intervals and level of activity of leg muscles in gait analysis [6]. In these applications, the surface EMG is mathematically described as colored noise, characterized by a probability density function (often Gaussian or Laplacian [12]). The main processing task is the estimation of the standard deviation or amplitude of this random process [10], [11].

Some applications of the surface EMG, mainly confined to academic laboratories, have made use of slightly more sophisticated processing methods with respect to amplitude estimation. For example, the power spectrum or time-frequency distribution of the EMG signal have been computed for inferring membrane properties of the active fibers during the development of muscle fatigue [15], [59], [64]. Other methods are based on spike analysis [40], fractal theory [71], high-order power spectral moments [65], and several variations of these techniques. However, these approaches have generally been proven to be limited when used to infer the neural

Manuscript received June 15, 2015; revised September 19, 2015; accepted October 27, 2015. Date of current version January 19, 2016. The work of D. Farina was supported by the European Research Council Advanced Grant DEMOVE (Contract 267888). The work of D. Farina and A. Holobar was supported by the Commission of the European Union, under the Framework 7 Grant Agreement ICT-2011.5.1-287739 "NeuroTREMOR: A novel concept for support to diagnosis and remote management of tremor." The work of A. Holobar was supported by the Slovenian Research Agency under the Grant Agreement "Definition of non-invasive marker for skeletal muscle atrophy: from validation to application" (Contract L5-5550).

D. Farina is with the Department of Neurorehabilitation Engineering, Bernstein Focus Neurotechnology Göttingen, Bernstein Center for Computational Neuroscience, Georg-August University of Göttingen, 37073 Göttingen, Germany (e-mail: dario.farina@bccn.uni-goettingen.de).

A. Holobar is with the Faculty of Electrical Engineering and Computer Science, University of Maribor, 2000 Maribor, Slovenia (e-mail: ales.holobar@um.si).

Digital Object Identifier: 10.1109/JPROC.2015.2498665

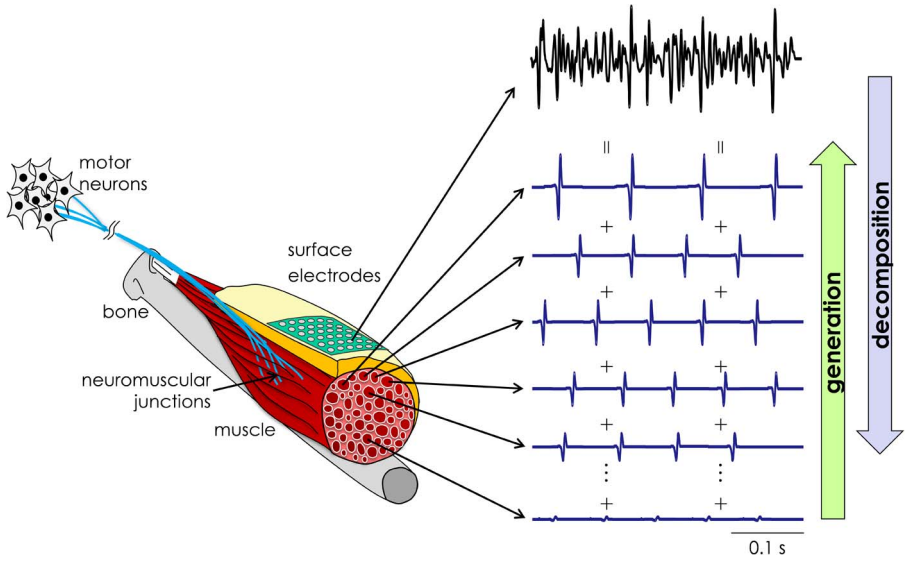

Fig. 1. ***Generation and decomposition of the surface EMG signal. Motor neurons in the spinal cord provide the neural drive for muscle fiber activation. The surface EMG is originated as the sum of the trains of MUAPs. Its decomposition consists in the mathematical derivation of the task of retrieving the trains of MUAPs from the interference signals.***

signals that the muscles receive to generate movements [28], [36]. The main reason for these limitations is that features extracted from the interference EMG are influenced by the properties of the action potentials (APs) of the active motor units [23], [27]. The motor unit APs (MUAPs) depend on the muscle and subject anatomy and on the muscle conditions. Comparison of EMG features among subject groups and conditions is therefore problematic. For example, the first-order moment, or mean frequency, of the surface EMG power spectrum is influenced by the fiber anatomy, the tissue filtering, the velocity of propagation of the APs, and the intracellular APs [21], [22]. Because it is not possible to define global signal features that are completely independent from the properties of the APs, the surface EMG has been traditionally considered as a crude means of investigating the neural mechanisms of muscle control [28], [36].

The approach of extracting global features from the interference EMG has been progressively substituted by a more detailed analysis of the signal. Initially, methods for increasing the selectivity of the recording have been proposed. With these techniques, it has been possible in early studies to identify single motor unit discharge patterns from raw EMG traces [62], [72], [73]. Although these studies did not propose a full surface EMG decomposition in general conditions, they contributed to changing the view of the processing of surface EMG signals. This view was changed from the extraction of features of a colored noise process to the identification of the individual sources that, when summed together, fully explain the signal generation. The latter approach, which is referred to as EMG signal decomposition, completely separates the neural information in the signal (i.e., the series of discharge timings of the active motor neurons) from the APs of the active motor units. The full surface EMG decomposition is the ultimate processing goal because it explains the signal into its most basic elements. In doing so, this analysis provides a noninvasive means for assessing the neural drive to muscles, i.e., the output from the spinal cord circuitries.

This review describes methods developed mainly in the last decade for estimating individual motor unit activities from the surface EMG.

II. SURFACE EMG SIGNAL GENERATION

Each muscle is innervated by a pool of motor neurons which provide the drive for muscle contraction. When an AP is conducted through the axon of a motor neuron and reaches the neuromuscular junction, an AP in each innervated muscle fiber is generated (Fig. 1). The sum of the APs of the muscle fibers innervated by a motor neuron (muscle unit) is a compound potential, also called MUAP.

The motor unit comprises the motor neuron and its innervated muscle fibers. It is the smallest functional element of the neuromuscular system that can be voluntary activated. Since the neuromuscular junction is an extremely reliable synapsis, there is a one-to-one correspondence between each motor neuron AP and the corresponding MUAP. Therefore, the muscle units act as biological amplifiers of the neural activity.

Fig. 1 shows the generation of the surface EMG signal as a sum of the MUAP trains. The decomposition of the

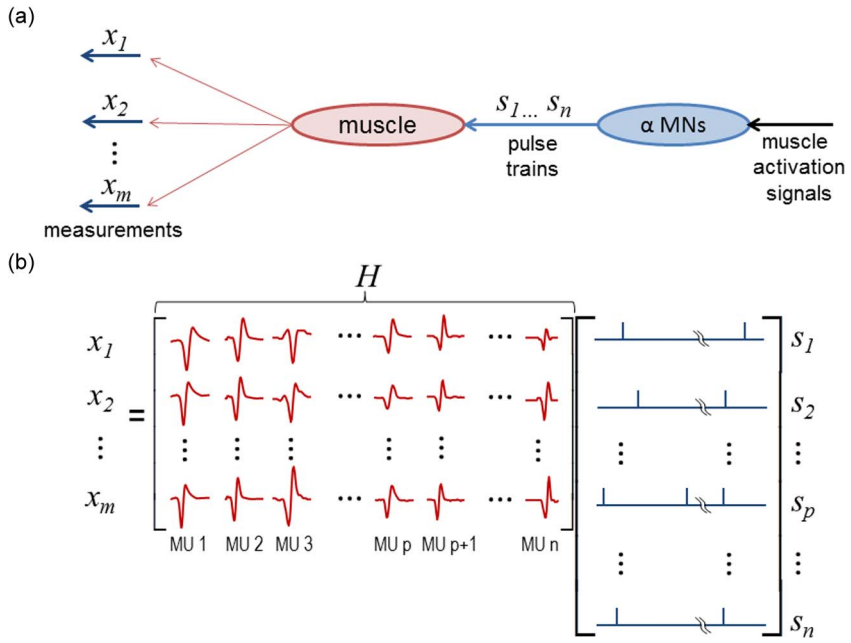

Fig. 2. ***Convolutive data model of surface EMG signals. (a) Motor neurons (MNs) drive the electrical activity of muscle fibers and motor units spatially spread and amplify the information about neural drive. (b) Activity of alpha motor neurons is modelled by series of discrete delta functions, representing the discharge times*** $s_i(k)$***. Motor units convolve these series of deltas with MUAPs. Volume conductor acts as a low-pass filter, thus MUAPs, measured by different uptake electrodes, differ considerably.***

surface EMG is the inverse process and consists in the extraction of the MUAP trains from the interference signal.

A. Mathematical Modeling

Based on its generation (Fig. 1), the EMG signal can be expressed by the following mathematical model [Fig. 2(a)]:

$$x_i(k) = \sum_{j=1}^{n} \sum_{l=0}^{L-1} h_{ij}(l) \sum_{r} \delta(k - \varphi_{jr} - l) + n_i(k), \quad i = 1, \ldots, m, \qquad k = 0, \ldots, D_R \tag{1}$$

where $x_i(k)$ is the ith EMG signal, recorded at location i (multichannel EMG recording), m is the number of locations over the muscle where the signal is recorded from, k is the discrete time, D_R is the duration of the recording (in samples), $h_{ij}(l)$ is the AP of the jth motor unit (peripheral properties) as recorded at the ith location, $\sum_r \delta(k - \varphi_{jr})$ is the spike train of the jth motor unit with spikes at times φ_{jr} (neural information), $n(k)$ is the additive noise, L is the duration of the APs, and n is the number of active motor units. Equation (1) represents a multiple-input–multiple-output (MIMO) system that can be viewed as m observations of a convolutive mixture of n sources (motor units) [47], [48]. This convolutive mixture can also be expressed in a compact matrix form. By indicating $s_j(k) = \sum_r \delta(k - \varphi_{jr})$, we can indeed write

$$\underline{x}(k) = \sum_{l=0}^{L-1} \underline{\underline{H}}(l) \underline{s}(k - l) + \underline{n}(k) \tag{2}$$

where $\underline{x}(k) = [x_1(k), x_2(k), \ldots, x_m(k)]^T$ is the matrix of m EMG signals (observations), recorded on the muscle and $\underline{s}(k) = [s_1(k), s_2(k), \ldots, s_n(k)]^T$ are the n motor unit spike trains (sources) that generate the EMG signals. The matrix $\underline{\underline{H}}(l)$ has size $m \times n$ and contains the lth sample of MUAPs for the n motor units and m channels.

The model of (2) can be interpreted as the mixture of sources represented by the series of discharge timings of the motor units filtered by unknown impulse responses (the APs). The sources are associated to the neural information of the signals and the filters correspond to the APs [Fig. 2(b)].

The convolutive mixture model of (2) and Fig. 2 can be also rewritten as an instantaneous mixture of an extended vector of sources that include the original sources and their delayed versions [46]–[49]. In this way, the new source vector after the extension has size $n \times L$, where L is the length in samples of the MUAPs. Often, the observations are also extended by delayed versions in order to keep the ratio between the number of observations and the number of sources as high as possible.

The extended observation vector for the channel j is as follows:

$$\widetilde{x}_j(k) = \left[x_j(k)x_j(k-1), \ldots, x_j(k-R)\right], \quad j = 1, \ldots, m$$

where R is the extension factor for the observations, typically set for EMG decomposition to values between 10 and 15. After the extension of the observations, we also have

$$\tilde{s}_i(k) = [s_i(k), s_i(k-1), \ldots, s_i(k-(L+R-1))], \quad i = 1, \ldots, n$$
$$\widetilde{n}_j(k) = \left[n_j(k), n_j(k-1), \ldots, n_j(k-R)\right], \quad j = 1, \ldots, m.$$

Therefore, we can define the extended model as [47], [48]

$$\underline{\widetilde{x}}(k) = \underline{\underline{\widetilde{H}}}\,\underline{\widetilde{s}}(k) + \underline{\widetilde{n}}(k), \qquad k = 0, \ldots, D_R \tag{3}$$

With

$$\underline{\widetilde{s}}(k) = [\widetilde{s}_1(k), \widetilde{s}_2(k), \ldots, \widetilde{s}_n(k)]^T$$
$$\underline{\widetilde{x}}(k) = [\widetilde{x}_1(k), \widetilde{x}_2(k), \ldots, \widetilde{x}_m(k)]^T$$
$$\underline{\widetilde{n}}(k) = [\widetilde{n}_1(k), \widetilde{n}_2(k), \ldots, \widetilde{n}_m(k)]^T$$
$$\tilde{h}_{ij} = \begin{bmatrix} h_{ij}[0] & \cdots & h_{ij}[L-1] & 0 & \cdots & 0 \\ 0 & \ddots & \ddots & \ddots & \ddots & \vdots \\ \vdots & \ddots & \ddots & \ddots & \ddots & 0 \\ 0 & \cdots & 0 & h_{ij}[0] & \cdots & h_{ij}[L-1] \end{bmatrix}$$
$$\underline{\underline{\widetilde{H}}} = \begin{bmatrix} \widetilde{h}_{11} & \cdots & \widetilde{h}_{1n} \\ \vdots & \ddots & \vdots \\ \widetilde{h}_{m1} & \cdots & \widetilde{h}_{mn} \end{bmatrix}.$$

The model of (3) represents a linear instantaneous mixture of sources that are the original series of motor unit discharge timings and their delayed versions. This compact model is shown in Fig. 2(b).

B. Properties of Motor Unit Spike Trains

In the model of (3), the sources to be estimated are the series of timings of activation of each motor unit $s_j(k) = \sum_r \delta(k - \varphi_{jr})$, $j = 1, \ldots, n$, as well as their delayed versions $s_j(k-p) = \sum_r \delta(k - \varphi_{jr} - p)$, $p = 1, \ldots, L+R-1$. Since they are the targets of EMG decomposition, it is useful to report some properties of these sources.

The random variables φ_{jr} are the timings of activation for the jth motor unit. Assuming that the motor units have a constant average interspike interval T_j and a variability of the interspike interval is represented by a zero-mean random variable θ_{jr}, the series of timing of activations can be expressed as

$$s_j(k) = \sum_r \delta(k - rT_j + \theta_{jr}). \tag{4}$$

Assuming that the variables θ_{jr} in (4) are uncorrelated and share the same probability density function $q_\theta(u)$, the series of timings in (4) is a wide-sense cyclostationary process with period T_j. This process can be characterized by averaging its periodic autocorrelation function. By assuming that the probability density function $q_\theta(u)$ is approximately null outside the interval $[-T_j/2, T_j/2]$, the averaged autocorrelation function of the process in (4) is

$$R_{s_j s_j}(k) = \frac{1}{T_j}\left[\delta(k) + \sum_{l \neq 0} R_\theta(k - lT_j)\right] \tag{5}$$

where $R_\theta(k)$ is the autocorrelation function of $q_\theta(u)$.

The power spectrum of the spike trains in (4) is obtained as the Fourier transform of the autocorrelation function [see (5)]

$$G_{s_j s_j}(f) = \frac{1}{T_j}\left[1 - G_q(f)\right] + \frac{1}{T_j^2} G_q(f) \sum_l \delta\left(f - \frac{l}{T_j}\right) \tag{6}$$

where $G_q(f)$ is the Fourier transform of $R_\theta(k)$.

Finally, we note that delayed versions of a source share the second-order statistical properties (autocorrelation function) and have thus the same power spectra.

Fig. 3 shows the autocorrelation function and power spectrum of series of discharge timings for a healthy subject and a patient suffering with essential tremor. The corresponding Fourier transforms are also shown (power spectra). The two examples correspond to very different statistics of discharge timings that are reflected in the second-order statistical description. In particular, the series of discharge timings in the essential tremor patient have very small discharge variability with respect to the healthy control.

C. Volume Conductor

The sources in the model of (3) represent the neural information in the surface EMG recording. Conversely, the filters $h_{ij}(l)$ in the same model are the jth MUAPs detected in each location of recording (ith channel) (Fig. 2).

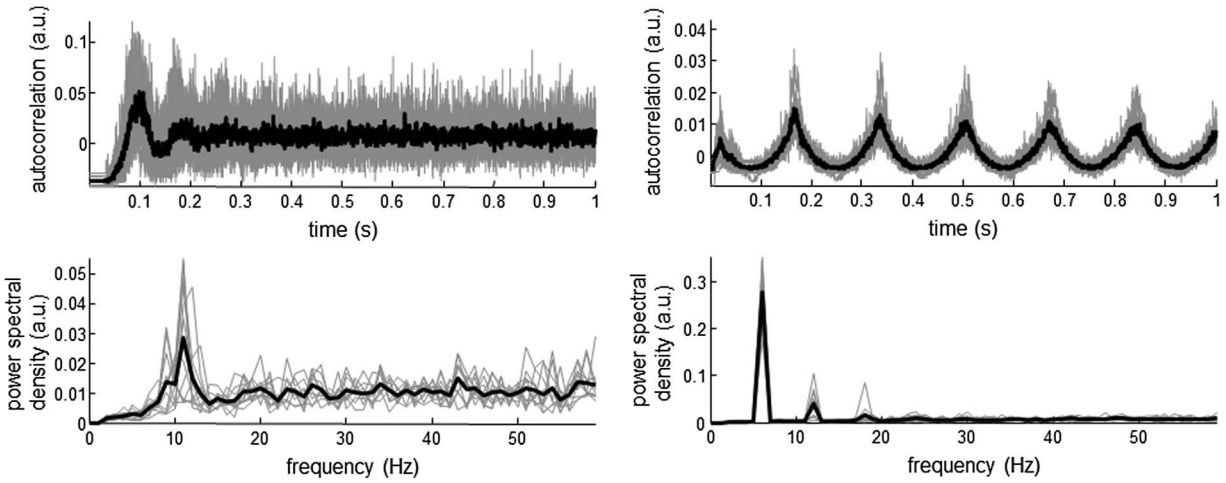

Fig. 3. *Autocorrelations and power spectral densities of the spike trains of 12 motor units identified in a young healthy subject (left) and 11 motor units identified in an elderly essential tremor patient (right) during moderate constant force isometric contraction. Only one second of autocorrelation function is depicted. Results from individual motor units are in gray, and the average values are in black.*

These filters represent the spatial distribution of electric potential generated by each motor unit (peripheral information). The latter depends on the electrical activity of the muscle fibers, the location of the muscle unit, as well as the properties of the tissues separating the fibers from the recording electrodes (the so-called volume conductor).

Under electrostatic conditions, for each instant, the electric potential detected in a location over the skin is the spatial convolution of the transfer function of the tissues and the current density of the depolarization zone of the muscle fibers. The effect of the volume conductor is therefore essentially a spatial filtering. The transfer function of the tissues can be computed analytically in simplified geometries, such as infinite volume conductors or planar/cylindrical layered tissues [5], [20], [26], [29], [44], or numerically in more general conditions [60]. Since in all cases the transfer function of the volume conductor corresponds to the Fourier transform of the spatial impulse response of a resistive medium that satisfies the Poisson's equation, the filtering effect is that of a low-pass system [59]. The selectivity of this filter depends on the physical characteristics of the tissues and the distance between the sources and the recording point. However, the volume conductor in surface EMG detection is a very selective filter. It decreases the bandwidth of the recorded potential from a few kilohertz in case of intramuscular recordings (with negligible effect of the volume conductor) to only 300–400 Hz for surface EMG recordings (Fig. 4).

The low-pass nature of the volume conductor has two main consequences on the detected potentials. First, the spatial distribution of surface potentials is very broad due to the decrease in spatial bandwidth. Therefore, several muscle units contribute to the recording from a specific location. This corresponds to a poor spatial selectivity of the recording. For this reason, with respect to intramuscular EMG, the surface EMG usually comprises the activity of a much greater number of motor units. Second, the low-pass spatial selectivity removes information on the shapes of the APs. This effect explains why surface APs of different motor units are usually very similar. This second problem has profound influence on the methods for decomposing the surface EMG since the model of (3) cannot be solved if the filters (APs) for the different sources are the same (as discussed in the section "V.A Full

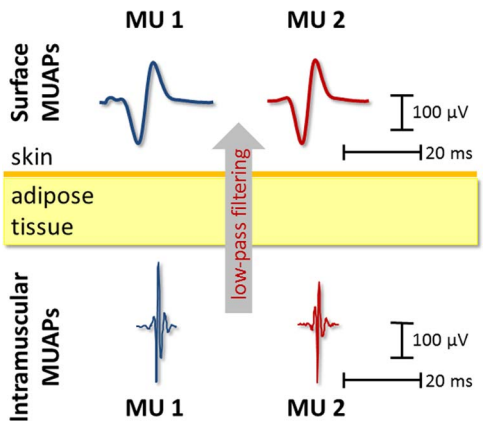

Fig. 4. *Comparison of intramuscular and surface MUAPs for two motor units identified from the biceps brachii muscle of a healthy young subject during an isometric contraction at 20% of the maximal force. Although the MUAPs differ substantially when recorded invasively (intramuscular EMG), they are almost identical when recorded noninvasively (surface EMG). This is due to the filtering effect of the volume conductor.*

decomposition: need for different convolutive filters"). These two effects are shown in Fig. 4 that reports the intramuscular and surface APs for two motor units. The intramuscular APs have substantially shorter durations (greater bandwidth) than their surface counterparts. Moreover, the two APs are clearly distinguishable from their waveforms when detected invasively while they are almost identical on the skin surface.

In addition to the influence of the volume conductor, the MUAP depends on the intracellular AP shape and on its velocity of propagation along the muscle fibers. For pure propagation at constant velocity, the duration of the surface AP is inversely associated to its velocity of propagation [59]. Because the power spectrum of the surface EMG has a bandwidth inversely related to the average AP duration, it has been used as an indicator of the membrane fiber properties [14]. However, despite the association between some physiological variables and the properties of the surface APs, the effect of the volume conductor on the APs (Fig. 4) has an important impact on methods used to extract global variables from the surface EMG [28], [36].

III. INDIRECT ESTIMATION OF MOTOR UNIT ACTIVITY

The global analysis of the EMG signal does not identify the motor units as different sources but rather aims at indirectly identifying associations between EMG features and some motor unit properties. For example, the amplitude of the signal is an estimate of the strength of the neural drive to the muscle, i.e., the number of APs discharged by the motor pool innervating the muscle.

From (1), neglecting the effect of the additive noise for simplicity, it is possible to derive the power spectrum $G_x(f)$ of a single-channel surface EMG signal as

$$G_x(f) = \sum_{j=1}^{n} G_{s_j s_j}(f) \cdot |H_j(f)|^2 \tag{7}$$

where n is the number of active motor units, $G_{s_j s_j}(f)$ is the power spectrum of the spike train of the jth motor unit, as obtained in (6), and $|H_j(f)|^2$ is the square magnitude of the Fourier transform of the AP of the jth motor unit. The derivation of (7) assumes uncorrelated sources (motor unit activities), as a first approximation. For typical values of the discharge rates and interspike interval variability, the dominant term in $G_{s_j s_j}(f)$ [see (6)] is the first, since the second is a series of delta functions modulated by the (low-pass) Fourier transform of the probability density function of the interspike interval variability. Moreover, the first term is constant and equal to $1/T_j$ for frequencies greater than 10–20 Hz. Therefore, the power spectrum of the EMG signal is approximately equal to the weighted sum of the energy spectra of the active motor unit APs, with the weights being the discharge rates

$$G_x(f) \cong \sum_{j=1}^{n} \frac{1}{T_j} \cdot |H_j(f)|^2. \tag{8}$$

From (8), the EMG signal power is obtained as follows:

$$P_x \cong \sum_{j=1}^{n} \frac{1}{T_j} \cdot En_j \tag{9}$$

where En_j is the energy of the AP of the jth motor unit. The signal amplitude is the standard deviation of the EMG signal that corresponds to the square root of the power

$$\sigma_x \cong \sqrt{\sum_{j=1}^{n} \frac{1}{T_j} \cdot En_j}. \tag{10}$$

Equation (9) indicates that the power of the EMG is a good approximation to the sum of the energies of the individual MUAPs, each multiplied by the corresponding discharge rate. Therefore, the power of the EMG increases monotonically when increasing the neural drive to the muscle, i.e., increasing the number of active motor neurons and frequency of motor neuron AP discharges. The intensity of muscle activity is thus associated in a monotonic way to the intensity of the neural signal sent from the spinal cord. However, from (9), the total power also depends on the distribution of energies of the APs, which is determined by volume conductor properties [27]. For this reason, the association between the power of the surface EMG and the neural drive to the muscle has a very large variability among conditions, tasks, muscles, and subjects. The same considerations hold for the signal amplitude provided in (10). Contrary to power, the amplitude is not preserved, i.e., the surface EMG amplitude is less than the sum of the constituent sources (AP trains). This effect has been referred to as amplitude cancellation and contributes to the variability of amplitude when changing the distribution of APs [13], [34], [57], [58].

Fig. 5 shows the estimated excitation to the muscle when running simulations that have the same discharge timings of all the active motor units (same neural excitation) but randomly varying the location of the motor units in the muscle tissue. With a simulated excitation level of 70% of the maximum, for example, the estimated amplitude level may vary from 60% to 90% of the maximum and this variability is exclusively due to the

different distribution of AP energies by randomly locating the muscle units within the muscle tissue.

Similar to the case of total signal power, the spectral analysis of the EMG signal approximately provides information on the frequency distribution of the power of the average MUAP [see (8)]. Since one of the factors that determine the duration of a MUAP is its velocity of propagation [59], variables associated to the EMG signal bandwidth (inversely related to the AP duration) have been used for inferring the average muscle fiber conduction velocity. This assumption has been applied in a variety of studies with different degrees of accuracy (see [76]). The main problem of the association is that another important factor influencing the AP duration is the volume conductor [32], through the discussed low-pass spatial filtering effect.

The dependence of EMG power and its frequency distribution on the MUAPs extends to any other global feature extracted from the surface EMG. These features intrinsically depend on all the factors by which the MUAPs are influenced. Therefore, global EMG variables usually provide a very crude association with the neural control strategies (behavior of motor units).

The methods based on the global analysis of the surface EMG do not separate the neural information (discharge timings) from the peripheral information (membrane properties and volume conductor) in the EMG signal. This separation is performed by decomposition methods.

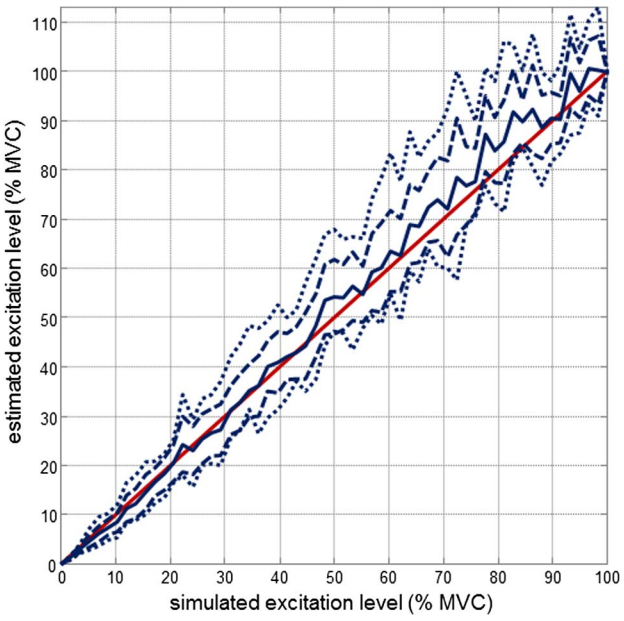

Fig. 5. *Excitation level as estimated by the average rectified value (ARV) metric (an estimator for signal amplitude) with window length of 250 ms applied to surface EMG signals simulated during a linearly increasing contraction with the excitation level ranging from 0% to 100% of the maximal force. The results are normalized to the ARV value at the maximal simulated excitation level and averaged over ten simulation runs with randomly distributed motor units within the muscle tissue in each run. The solid blue line indicates the average value, the dashed blue lines indicate the standard deviation, and the dotted blue lines indicate the maximal and minimal values of estimated excitation level across all simulation runs. Exactly the same motor unit firing patterns have been simulated in all the simulation runs. The variability is solely due to the distribution of motor units within the muscle tissue that determines different distribution of MUAP sizes.*

IV. INCREASING SELECTIVITY: SPATIAL FILTERING

One of the first attempts to identify individual motor unit activities from the surface EMG was based on the concept of increasing the spatial selectivity of the recordings. This would decrease the number of motor units contributing in each recording point. In this condition, the number of detected units may be sufficiently small for their direct identification.

Increasing the spatial selectivity can be achieved by high-pass spatial filtering. High-pass filters are edge detectors in image processing and partly compensate for the low-pass filtering effect of the volume conductor [72]. Spatial filtering in EMG recording is performed by deriving the weighted summation of the signals recorded by electrodes in different locations over the skin surface. These filters are necessarily finite impulse response (FIR) filters. Their transfer function can be designed on the basis of the set of weights given to each electrode and on the geometrical arrangement of the electrodes.

A single differential filter (or bipolar derivation) is the simplest high-pass spatial filter and corresponds to the spatial discrete operator for the first derivative. It enhances the local spatial variations and attenuates the global changes in space. The double differential filter corresponds to the discrete second derivative and the Laplacian filter to the discrete Laplacian operator (sum of the second-order partial spatial derivatives in the two directions of the skin plane) [72], [73]. In addition to these derivative operators, other filters, introduced in the field of image processing [24] or custom-designed for EMG applications [25], have been proposed. The selectivity of these filters depends both on the weights assigned to each electrode location and on the distance between electrodes (usually one distance defines the full geometry) [72], [73]. Selective 2-D spatial filters with small interelectrode distance may allow in some cases the extraction of the entire spike trains of single motor units at low to moderate contraction forces [62], [69], [70].

Interestingly, spatial filters for surface EMG signal detection, such as those here described, are spatial operators with similar characteristics as those used in EMG decomposition to directly separate the motor unit activities. However, rather than being signal dependent and

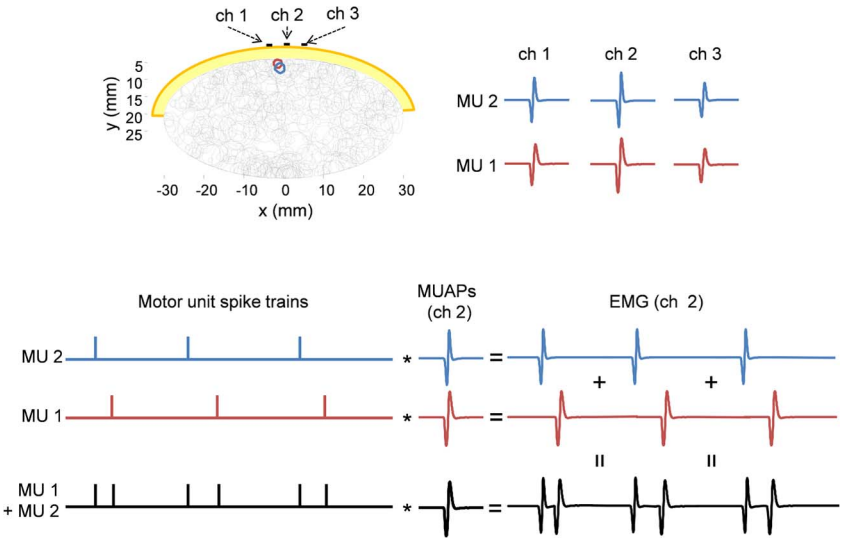

Fig. 6. ***MUAPs of two superficial motor units as detected by three bipolar surface electrodes (black rectangles in the upper left panel). The two motor units are of similar size and share almost the same location within the simulated muscle tissue. Thus, their MUAPs are almost identical (upper right panel). The signal generated as sum of the two trains of MUAPs of these two units is very similar to that generated by the sum of the two series of discharges convoluted by the common MUAP (one source). Thus, the two motor units cannot be distinguished and reliably identified by surface EMG decomposition (lower panel).***

designed to invert the model of (3), generic spatial filters are fixed 2-D FIR high-pass filters. These generic filters have a much smaller number of coefficients than the blind source separation (BSS) filters.

V. FULL DECOMPOSITION

A. Need for Different Convolutive Filters

The generic spatial filters proposed for increasing spatial selectivity may allow in specific cases to identify individual motor units. However, they cannot be used as decomposition methods, i.e., as methods to extract the individual motor unit contributions to the EMG signal in general conditions.

A full decomposition of the signal, i.e., the separation of the MUAP trains mostly contributing to the signal, requires the inversion of the model of (3). This model indicates that if two sources (series of delta functions representing the timings of activations of the muscle fibers) share the same filters (multichannel APs) they are indistinguishable. Indeed, in this situation, the presence of two series of delta functions convoluted by the same filter and summed together (two sources) is equivalent to the sum of the two series of deltas convoluted by the filter (one source). Therefore, the decomposition is theoretically not possible if two or more motor units to be identified have exactly the same APs. A necessary condition for decomposition is that the multichannel APs of all motor units to be identified are unique, i.e., not shared by other units [33]. Fig. 6 shows two motor units whose simulated APs recorded from three channels (observations) are almost identical. This is due to the fact that, in this example, the two units are similar in size and in location into the volume conductor—a situation that can often occur experimentally. The signal generated as sum of the two trains of APs of the two units (two sources) is obviously very similar to that generated by the sum of the two series of discharge timings convoluted by the common AP (one source). It is not possible to distinguish the two conditions (one source versus two sources) in this situation, especially with high physiological noise, i.e., large contributions of other motor units that are active in the muscle tissue.

The uniqueness of APs of the motor units to be identified is a necessary condition for decomposition, not linked to a specific decomposition approach [33]. Because the volume conductor separating muscle fibers from the electrodes reduces substantially the signal bandwidth, it is very likely that APs of different motor units are similar when detected in one single or few locations. This has been shown with simulation analyses [33]. However, the larger is the number of recording locations, the lower is the likelihood that the detected multichannel APs are similar among motor units. This intuitive property has been tested extensively in simulated conditions [33]. The simulations proved that full decomposition of the signal is theoretically not possible in generic conditions if done from less than 30–40 EMG channels. Therefore, electrode systems providing a large number of EMG channels (high-density EMG) are most suited for full decomposition.

B. Need for BSS Methods

The classic approach to the decomposition of intramuscular EMG signals has been the segmentation and classification of the signal segments, with the usual addition of the resolution of superimposed MUAPs [74]. This procedure is obviously possible when the number of superimposed MUAPs is relatively small with respect to the number of isolated MUAPs. When this condition is met, probability of detecting isolated MUAPs for each source to be identified is relatively high. The superimpositions are then resolved with the knowledge of the contributing MUAP shapes.

While a typical intramuscular EMG signal has a relatively small percentage of potentials overlapped in time, in similar conditions a corresponding surface EMG signal shows a much greater proportion of overlaps [36]. Moreover, the MUAPs detected intramuscularly have greater bandwidth than their surface counterparts. They can be therefore better discriminated between motor units and, contrary to the surface MUAPs, they have already been used for diagnostic purposes [74].

Simple calculations [3], [36] show that the number of overlaps in surface EMG is so large that attempts based on segmentation and classification of MUAPs are likely deemed to fail. It is obvious that there will be special conditions in which the surface EMG signal can be decomposed with this approach, as we have seen with some examples of highly selective spatial filters, but these conditions are limited and do not generalize.

The above consideration implies that surface EMG decomposition requires the use of methods that are not influenced by the temporal overlapping of MUAPs and that estimate, in one step, the full set of timings of each motor unit. Moreover, these methods should rely on almost no *a priori* information since in general experimental conditions this is not available. Methods characterized by these properties are those of BSS [55], [56].

C. Separation Filters: Blind Source Separation

The model of (3) is that of a linear instantaneous mixture of sources represented by the series of discharge timings of each motor unit and their delayed versions. This model can be inverted, thus identifying the sources, with approaches that usually require that the sources are independent [e.g., independent component analysis (ICA)] or uncorrelated [e.g., second-order blind identification (SOBI)] and that the observations are at least as many as the sources [55], [56]. For the extended model, the latter property is verified if the original number of observations (without extension) is greater or equal than the original number of sources (without extension) and if $mR \geq n(L+R)$. In practice, however, any decomposition method aims at the separation of the sources that contribute with the majority of the energy to the observations. The other sources are not identified and contribute to the noise in the model of (3). Therefore, the condition of greater number of observations than sources is practically always verified by identifying only a subset of sources. The smaller is the subset of identified sources, the greater is the noise level that the decomposition method faces.

During voluntary contractions of nonfatigued healthy muscles, the motor unit discharge timings are pair-wise uncorrelated or only weakly correlated. Moreover, the extension of the source vector to the delayed version of the sources [see (3)] does not introduce correlation for small time lags, as shown briefly in the following.

Since the cross-correlation function between a source and its delayed version is the autocorrelation function of the source delayed by the imposed delay, the correlation matrix of the extended sources can be written as (11), shown at the bottom of the page [45]–[47].

This matrix is diagonal for small time lags, between 0 and $L+R-1$. Indeed, for nonzero time lags of up to $L+R-1$, the autocorrelation function of the generic source j is approximately [see (5)]

$$R_{s_j s_j}(k) \cong \frac{1}{T_j} R_\theta(k - T_j) \tag{12}$$

where $R_\theta(k)$ is the autocorrelation function of the probability density function of the interspike interval variability. If $L+R-1 < T_j$, the maximum value of $R_{s_j s_j}(k)$ for

$$\underline{\underline{R}}_{\underline{\underline{s}}\,\underline{\underline{s}}}(0) = \begin{bmatrix} \underline{\underline{R}}_{s_1 s_1}(0) & \cdots & \underline{\underline{R}}_{s_1 s_1}(L+R) & & & & \\ \vdots & \ddots & \vdots & \cdots & & 0 & \\ \underline{\underline{R}}_{s_1 s_1}(L+R) & \cdots & \underline{\underline{R}}_{s_1 s_1}(0) & & & & \\ & \vdots & & \ddots & & \vdots & \\ & & & & \underline{\underline{R}}_{s_n s_n}(0) & \cdots & \underline{\underline{R}}_{s_n s_n}(L+R) \\ & 0 & & \cdots & \vdots & \ddots & \vdots \\ & & & & \underline{\underline{R}}_{s_n s_n}(L+R) & \cdots & \underline{\underline{R}}_{s_n s_n}(0) \end{bmatrix} \tag{11}$$

$k = 1, \ldots, L + R$, is for $k = L + R$. This value is approximately null if $L + R$ is small with respect to T_j and if the variability of motor unit discharges is small. This is due to the fact that the time support of $R_\theta(k)$ is directly related to the variability of the discharge interval. Finally, if $L + R$ is within the absolute refractory period of the motor units (which is equivalent to assume a truncated probability density function $q(u)$), then $R_\theta(k)$ is *exactly null* for $k = 1, \ldots, L + R$. Therefore, the correlation matrix of the extended sources can be considered practically diagonal when the original sources are uncorrelated.

Contrary to correlation, the delayed versions of motor unit activation timings are by definition always mutually dependent, since a motor unit discharge cannot appear within the refractory period of the previous discharge. Thus, a spike in $s_j(k)$ is always followed by several zeros, meaning that, for small delays, a delayed version of $s_j(k)$ will always be equal to zero at the times of discharge of the original source $s_j(k)$. Nevertheless, independence is not necessarily needed for surface EMG decomposition (see below).

Because of the properties of the series of discharge timings of motor units, the model in (3) represents a linear instantaneous mixture for which the sources are uncorrelated (if the original sources were uncorrelated) and for which the number of observations is greater than the number of sources when the condition $mR \geq n(L + R)$ is met. A classic approach to source separation in these conditions is to first whiten the observations and then rotate them [55], [56]. A spatial whitening matrix $\underline{\underline{W}}$ makes the extended observations uncorrelated and of equal power. Therefore, its application to the extended observations $\underline{\tilde{x}}(k)$ provides

$$\underline{z}(k) = \underline{\underline{W}}\,\underline{\tilde{x}}(k) \tag{13}$$

in which $\underline{z}(k)$ has a covariance matrix equal to the identity. To verify (13), the whitening matrix should satisfy the following equation:

$$\underline{\underline{W}} = \underline{\underline{U}}\,\underline{\underline{D}}_S^{\gamma} \tag{14}$$

with $\gamma = -1/2$, and where $\underline{\underline{U}}$ is the diagonalization matrix of the covariance matrix of the extended observations (obtained, for example, by singular value decomposition)

$$\underline{\underline{R}}_{\tilde{x}\tilde{x}} = \underline{\underline{U}}\,\underline{\underline{D}}_S\,\underline{\underline{U}}^T \quad \text{with} \quad \underline{\underline{R}}_{\tilde{x}\tilde{x}} = E\left\{\underline{\tilde{x}}(k)\underline{\tilde{x}}^T(k)\right\} \tag{15}$$

with E standing for mathematical expectation.

The sources can be retrieved after whitening by finding the correction rotation (unitary) matrix to transform the whitened observations into the estimated sources. This matrix can be obtained by iterative procedures. A classic ICA approach can, for example, solve the problem, despite the violation of the independency condition [8]. This is due to the specific properties of spike trains and their delayed versions, as discussed in the following.

In the ICA approach, each source is extracted by projecting the extended, whitened observations on the separation vector w (one for each source)

$$\tilde{s}_j(k) = w_j\underline{z}(k). \tag{16}$$

Fig. 7 shows this procedure.

The separation vector w can be obtained iteratively with numeric minimization of a predefined cost function. For example, the fixed-point algorithm [55] provides the separation vector from the following iteration:

$$w_{\text{new}} = E\left\{g\left[w_{\text{old}}^T\underline{z}\right]\underline{z}\right\} - Aw_{\text{old}}, \quad \text{with } A = E\left\{g'\left[w_{\text{old}}^T\underline{z}\right]\right\} \tag{17}$$

where E stands for mathematical expectation. Additional normalization of w_{new} is needed after each iteration in order to prevent the convergence of source separation to trivial solutions. In classic ICA, the separation vector w maximizes the non-Gaussianity of the extracted source to separate it from the other sources. For independent sources, according to the central limit theorem and under the assumption of non-Gaussianity, the distribution of the sum of the sources is closer to the Gaussian distribution than the distribution of any individual source. Therefore, for independent sources, the separation vector w creates such a linear combination of whitened observations z, so that the contributions of all other sources but one are cancelled out, increasing the non-Gaussianity of w^Tz. Typically, the updating function $g(s)$ in (17) is set to $\tanh(s)$ or $s \cdot \exp(-s^2/2)$, representing the $\log(\cosh(s))$ and $\exp(-s^2/2)$ cost function for maximization of non-Gassianity, respectively [56]. We will discuss below that the same iteration and cost functions of the classic ICA approach can be applied to delayed spike trains which are not independent of each other, because of the sparseness of these spike trains.

Within this separation scheme, the convolution kernel compensation (CKC) approach [47], [48] has been the first convolutive BSS algorithm to be proposed and extensively tested for decomposition of multichannel EMG signals [50], [51]. Within the scheme of (17), instead of

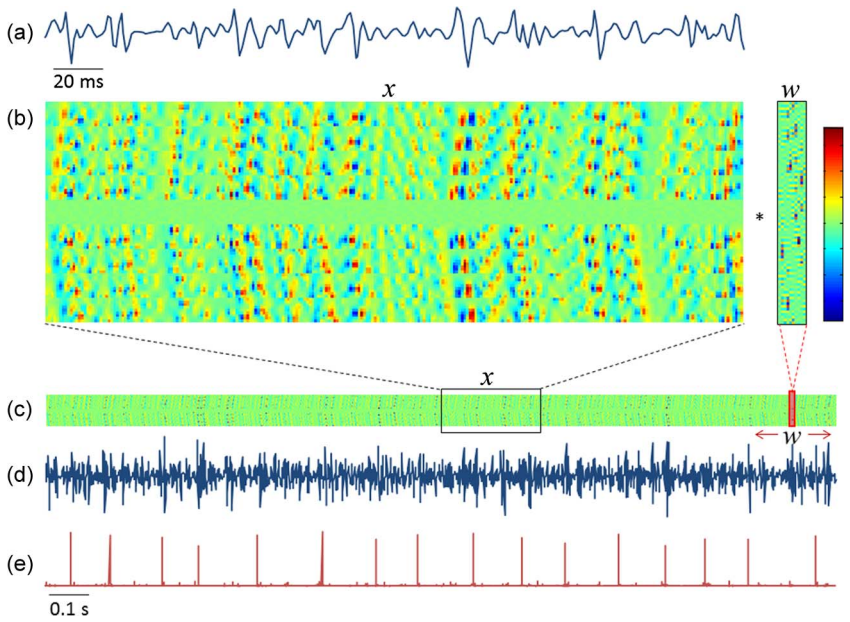

Fig. 7. *General scheme of BSS-based single motor unit spike train identification from multichannel surface EMG. (c) Eighty one color-coded channels of surface EMG recorded by 9 × 9 surface electrodes and reshaped into 81×K matrix of observations x, where K stands for the number of samples. (d) A single surface EMG channel [the 25th row of the matrix x in panel (c)]. Panels (a) and (b) are zoomed versions of (c) and (d). (e) Motor unit spike train as estimated by applying the source separation operator w [right-hand side of panel (b)] to the observation matrix x in (c). The kth sample of the motor unit spike train is estimated by aligning the left edge of the operator w with the kth column of the matrix x and summing up the element-wise product of w and x. This operation is equivalent to multiplying the extended observations with the separation vector w in (16).*

estimating the separation vector w directly, the CKC aims at the blind estimation of the cross-correlation vector $r_{\tilde{s}_j\tilde{x}}$ among the jth source $\tilde{s}_j(n)$ and all the observations $\tilde{x}(n)$ and uses it to estimate the jth source

$$\hat{s}_j(k) = r_{\tilde{s}_j\tilde{x}}^T R_{\tilde{x}\tilde{x}}^{-1}\tilde{x}(k) = r_{\tilde{s}_j\tilde{s}}^T \tilde{H}(\tilde{H}R_{\tilde{s}\tilde{s}}\tilde{H}^T)^{-1}\tilde{H}\tilde{s}(k) = r_{\tilde{s}_j\tilde{s}}^T R_{\tilde{s}\tilde{s}}^{-1}\tilde{s}(k). \quad (18)$$

With this iteration, the separation vector w in the scheme of (17) can be expressed as $w = r_{\tilde{s}_j\tilde{x}}^T R_{\tilde{x}\tilde{x}}^{-1}$ and, in the CKC approach, it is applied directly to the extended EMG observations $\tilde{x}(k)$ rather than to the whitened observations. The CKC approach utilizes the properties of the spike trains in the EMG signals to properly initialize the unknown separation vector $r_{\tilde{s}_j\tilde{x}}$ and, afterwards, optimizes it either by probabilistic framework approach or by gradient-based optimization, similar to the one discussed in the previous paragraph. The CKC iteration scheme is shown in Fig. 8.

The iterative scheme of (17) has been shown to provide accurate estimates of the sources in the surface EMG [8], [50], despite the fact that the independence property is not met for delayed versions of the same source. Fig. 9 explains why methods based on the optimization in (17), which is a typical ICA framework, also work for delayed trains of discharge timings when the independency assumption is in principle violated. In Fig. 10, the sparse source $s_1(k)$, simulating the motor unit discharge pattern (discharge rate of 15 Hz, 20% interspike variability) and its delayed version $s_1(k+1)$ have been mixed together into an observation $x(k) = a_1 s_1(k) + a_2 s_1(k+1)$, with mixing coefficients constrained to the unit circle $\sqrt{a_1^2 + a_2^2} = 1$. For each possible selection of coefficients a_1 and a_2, the $\log(\cosh(x))$ cost function [corresponding to $g(s) = \tanh(s)$ update function in (17)] was applied directly to the mixture x, as a measure of its non-Gaussianity. As can be observed in Fig. 9, despite the fact that the two sources considered are not independent, the $\log(\cosh(x))$ cost function attains its minima when one of the coefficients a_1 and a_2 is zero. Therefore, source separation is possible for these *dependent* (delayed) spike sources. In this way, it is possible to use the same optimization criteria and cost functions as in the ICA approach, since the sum of delayed *sparse* spike trains is closer to the Gaussian distribution than the distribution of the individual spike trains, even without the independence property.

At each optimization iteration, the estimated sources may be subtracted from the observations (peel-off approach) in order to increase the total number of

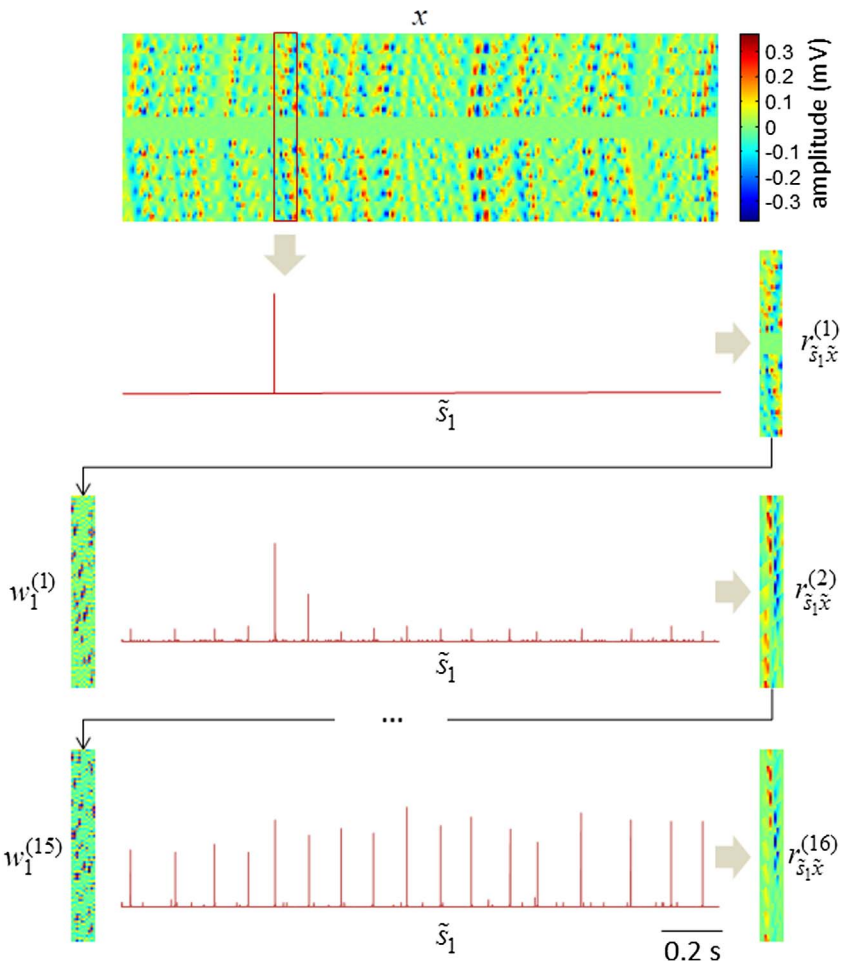

Fig. 8. ***Multiple iterations of CKC method for identification of single motor unit spike trains. Decomposition starts by approximating the cross-correlation vector $r_{\tilde{s}_1\tilde{x}}$ between the source $\tilde{s}_1(n)$ and all the extended observations $\tilde{x}(n)$. Afterwards, the separation vector is estimated as $w_1 = r^T_{\tilde{s}_1\tilde{x}} R^{-1}_{\tilde{x}\tilde{x}}$ and applied to the extended EMG observations $\tilde{x}(k)$ to yield a new estimate of the source $\tilde{s}_1(n)$. This procedure is then repeated until the algorithm converges to the final solution (superscripts in the brackets denote the decomposition iteration). The same approach is used for identification of other identifiable motor units.***

estimated sources [8] and prevent the convergence to already identified sources. However, this approach is prone to the accumulation of errors from previously identified sources [80]. Alternatively, it is possible to employ so-called source deflation procedures to decorrelate the estimated separation vectors and prevent the convergence to already identified sources [56], [80]. In this way, a relatively large number of motor units can be identified. For example, up to 53 simultaneously active motor units have been identified by the CKC method from 64-channel surface EMG recorded in isometric muscle contractions, and these numbers are likely to increase in the near future.

D. Effect of Synchronized Sources

The generation of muscle force requires that motor neurons receive common synaptic input [37], [38]. Therefore, their output spike trains are not fully uncorrelated. Nonetheless, the level of correlation between pairs of motor unit spike trains is small, even for a large amount of common input [38]. This is due to the nonlinear processing of input by motor neurons [36]. The small level of correlation between motor unit discharge timings in physiological conditions has been shown not to substantially hinder the possibility of surface EMG decomposition by ICA approaches [8]. However, there are pathological conditions in which the level of correlation may be very high. For example, in pathological tremor most of the motor unit discharges in each tremor burst occur at the same time [41], [52]. With respect to classic ICA-based methods [see (17)], the CKC approach for decomposition has been shown analytically and experimentally to be almost uninfluenced by the level of motor unit synchronization and, thus, by the degree of motor unit discharge dependences [52]. This is due to the fact that $r^T_{\tilde{s}_j\tilde{x}} R^{-1}_{\tilde{x}\tilde{x}}$ equals to the unity vector

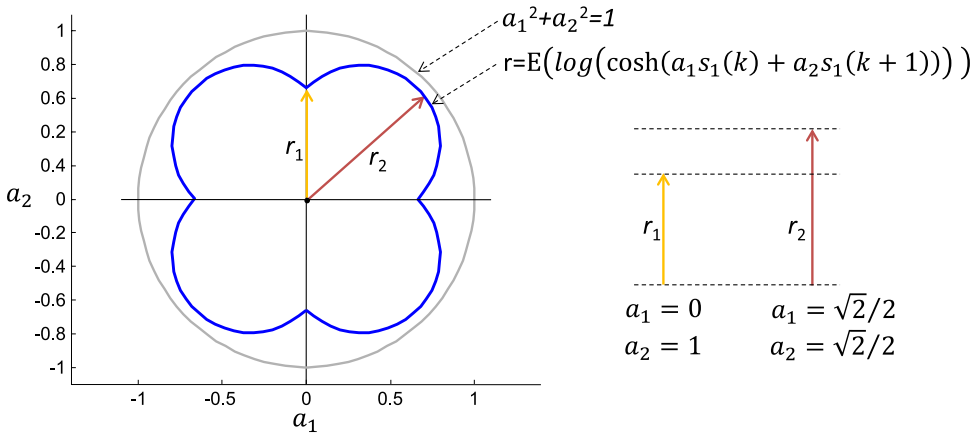

Fig. 9. ***Blind separation of mixtures of delayed spike trains. Sparse spike train $s_1(k)$, simulating the motor unit discharge pattern (discharge rate of 15 Hz, 20% interspike variability) and its delayed version $s_1(k+1)$ have been mixed together into an observation $x(k) = a_1 s_1(k) + a_2 s_1(k+1)$, with mixing coefficients constrained to unit circle $\sqrt{a_1^2 + a_2^2} = 1$. For each possible selection of coefficients a_1 and a_2, the $\log(\cosh(x))$ cost function [corresponding to $g(s) = \tanh(s)$ update function in (17)] was applied to x as a measure of its non-Gaussianity. Its value was plotted as a distance from the coordinate origin in the joint vector space of a_1 and a_2 coefficients (blue line). The $\log(\cosh(x))$ cost function clearly attains its minimums when one of the coefficients a_1 and a_2 is zero, i.e., when $x = \pm s_1(k)$ or $x = \pm s_1(k+1)$, indicating that the optimization procedures presented in (17) and (18) can also be applied to the mixtures of delayed spike series from the same motor unit, despite their statistical dependence.***

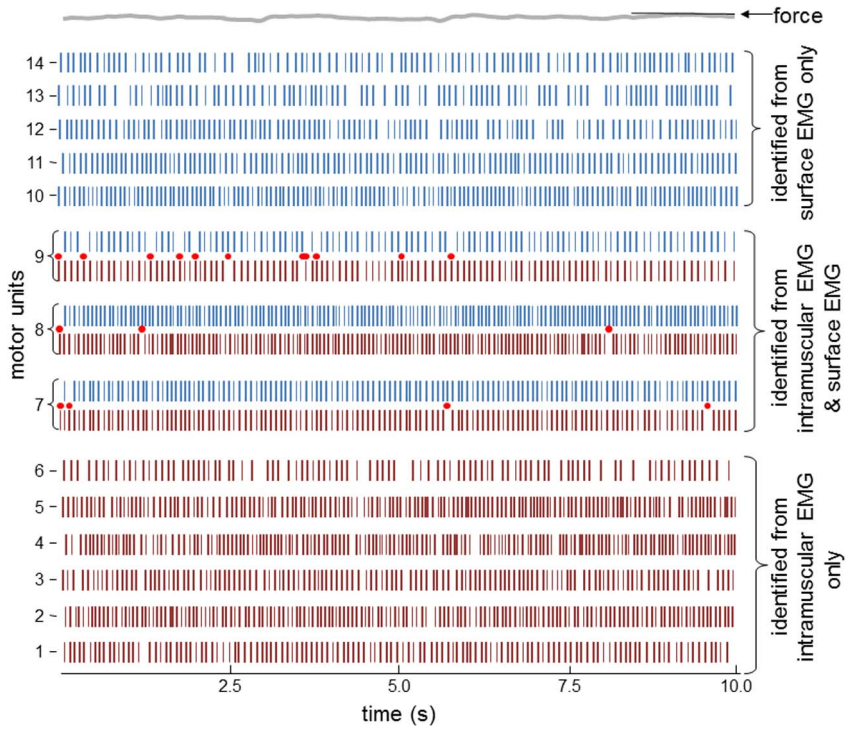

Fig. 10. ***Discharge times of motor units identified from intramuscular and surface EMG of the biceps brachii muscle during an isometric, constant force contraction at 5% MVC. Each vertical line indicates a motor unit discharge at a given instant. Motor unit discharge patterns, identified from surface EMG, are depicted in blue, whereas the discharge patterns identified from intramuscular EMG are in red. The motor units #7, #8, and #9 were identified from both surface and intramuscular EMG. The discharge patterns of these three units are depicted twice, once for surface and once for intramuscular EMG decomposition. The disagreements between these decompositions are depicted by red circles. Reprinted with permission from [51].***

with a single nonzero element at the jth position, regardless of the level of motor unit synchronization (except the case of 100% motor unit synchronization, i.e., when all the discharge timings of one source correspond exactly to the discharges of the other source, down to the discharge times tolerance of one sample). The exact proof of the CKC convergence in the case of synchronized motor units is out of the scope of this review and can be found in [52]. In intuitive terms, the sum of sparse motor unit spike trains is less sparse than the individual spike trains in all cases, except when the two spike trains are identical and all MUAPs occur at the same time instants [80].

E. Online Tracking of Motor Unit Activities

In some applications, it is desirable to perform a full EMG decomposition online. This is relevant, e.g., in biofeedback applications where the activities of individual motor units are displayed to a subject who is asked to modulate them voluntarily. Online decomposition is not possible for methods based on segmentation, classification, and resolution of superimpositions but, conversely, it is feasible, with appropriate computational means, for BSS-based methods.

The CKC decomposition algorithm, for example, has been recently implemented in an online fashion [43]. The online CKC decomposition consists of two steps. In the first, so-called calibration step, the separation vectors $w = r_{\tilde{s}_j\tilde{x}}^T R_{\tilde{x}\tilde{x}}^{-1}$ of different motor units are blindly estimated on a set of ~10-s-long observations $\tilde{x}(k)$ [43]. In the second step, which is performed online, the cross-correlation matrix of the observations is first updated as $R_{\tilde{x}\tilde{x},\text{new}} = R_{\tilde{x}\tilde{x},\text{old}} + E(\tilde{x}(k_{\text{new}})\tilde{x}^T(k_{\text{new}}))$ where $\tilde{x}(k_{\text{new}})$ denotes the new observation samples and then the separation vectors are updated as $w_{\text{new}} = r_{\tilde{s}_j\tilde{x},\text{old}}^T R_{\tilde{x}\tilde{x},\text{new}}^{-1}$ and new samples of motor unit spike trains are estimated as $\tilde{s}_j(k_{\text{new}}) = w_{\text{new}}^T\tilde{x}(k_{\text{new}})$. Finally, $r_{\tilde{s}_j\tilde{x}}^T$ is updated as $r_{\tilde{s}_j\tilde{x},\text{new}}^T = r_{\tilde{s}_j\tilde{x},\text{old}}^T + E(\tilde{s}_j(k_{\text{new}})^T\tilde{x}(k_{\text{new}}))$. All these updating steps can be performed highly efficiently and require ~20% of processing time on a standard single core personal computer processor [43]. When required, the old observation samples can also be removed from $r_{\tilde{s}_j\tilde{x}}^T$ and $R_{\tilde{x}\tilde{x}}$, supporting the tracking of dynamic changes in MUAPs.

F. Validation of Decomposition

As for any algorithm, surface EMG decomposition requires an extensive validation for its results to be accepted by the scientific community. Validation of surface EMG decomposition, however, is a challenge. The main issue is that the surface EMG cannot be manually decomposed by an expert since it is not possible to identify the individual motor unit contributions from the interference surface signal. This is due to the poor spatial selectivity of the surface EMG, as discussed above. Therefore, the manual decomposition by experts, which is often used as a validation method for intramuscular EMG decomposition, is not a viable means for validating surface EMG decomposition.

An obvious way to validate surface EMG decomposition consists in generating simulated signals for which the sources are fully known [50]. This is limited with respect to the test on experimental signals, yet it is a needed first step. Indeed failure on simulated signals would imply the need to refine the method before proceeding with experimental signals. Models for surface EMG generation [5], [29] and for motor neuron activation [9] are now very advanced and their simulated signals mimic very closely the experimental signals. The main advantage of the use of simulated signals for validation is that the ground truth is known. For this reason, it is possible to report the accuracy as a function of a number of factors of influence, such as signal-to-noise ratio, that can be easily varied in a large set of simulations.

Validation on experimental signals requires relative comparison of decomposition results. A classic approach of this type is to record intramuscular EMG signals concurrently with the surface EMG and decompose them by different methods. When the surface and intramuscular EMG share at least one source (motor unit activity) recorded by both systems, the decomposition results can be compared for the sources that both methods identify. For these sources, mismatches between the two methods are considered conservatively errors while agreements are considered correct decomposition instances. These assumptions are based on the fact that if two independent methods applied to different signals agree on a decomposition result, then this result is very likely correct. It would be extremely unlikely for the two methods to make the exact same mistake. For this reason, this comparison (intramuscular versus surface EMG decomposition) does not consider the intramuscular EMG decomposition as the gold standard, but rather both methods are validated against each other, without any one being the reference. The error rate estimated with this procedure is likely greater than the error rate of each of the two methods since error counting sums together the errors of both methods (the estimated error rate is close to the sum of the two error rates). Fig. 10 shows this validation approach.

The comparison of intramuscular and surface EMG decomposition is one possible version of a more general approach that is usually termed "two-source validation" [61]. The original proposal consisted in the validation of intramuscular EMG decomposition by computing the rate of agreement between decomposition results of two intramuscular signals that shared some sources. The same approach can be also applied to two surface EMG signal decompositions [17]. However, the two-source validation is appropriate only if applied to signals that share a minimal number of sources and for the rest they are independent. Indeed, at the extreme case, if the two signals are very similar (and are decomposed with the same

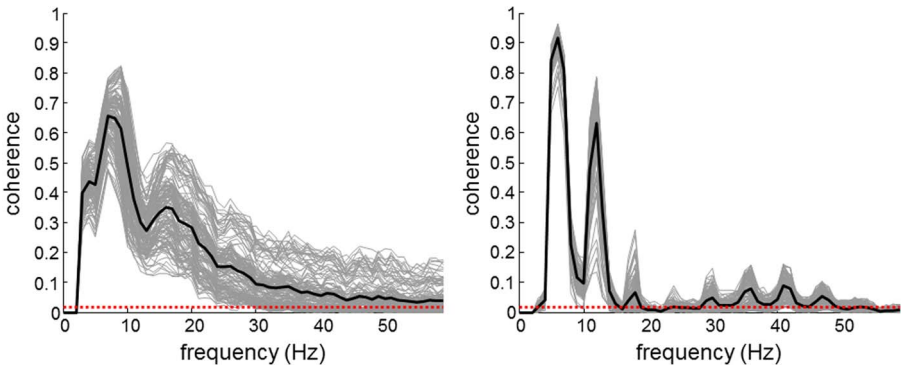

Fig. 11. *Coherence functions between the cumulative spike trains of 12 motor units identified in a young healthy subject (left) and 11 motor units identified in an elderly essential tremor patient (right). The plots show the coherence spectra for all possible pairs of cumulative spike trains computed from two complementary sets of five randomly selected motor unit spike trains (in gray). Their mean value is depicted by a solid black line. The dashed red line depicts the 99% confidence level.*

method), the two decompositions will be very similar regardless of the accuracy of the decomposition.

In addition to the model-based and the two-source approach, other methods have been recently proposed for validating surface EMG decomposition. For example, Holobar *et al.* [53] derived a computationally highly efficient pulse-to-noise ratio (PNR) index. This index expresses the signal-to-noise ratio in the identification of each source (motor unit discharge timings) and proved to be highly correlated with the decomposition accuracy [53]. Other authors have proposed further ideas for validation [54], [67]. Since the topic is central in this area, it is not surprising that some of these validation approaches have generated a debate on their appropriateness [18], [19], [35], [36], [39].

VI. IDENTIFICATION OF COMMON INPUT TO MOTOR NEURONS

Surface EMG signal decomposition provides a window into the outputs of the motor neurons pools. The analysis of these output signals provides information on the synaptic input that the motor neurons receive, spinally and supraspinally. The single motor neurons operate nonlinearly and therefore it is difficult to estimate their input from the output. Nonetheless, the motor neuron pool is approximately linear [36]–[38], [68]. Each motor neuron presents at least two components in its output spike train [38]: the component due to the actual input it receives and the component generated by the motor neuron nonlinearity. The input component is further divided into the component due to an input signal shared by all motor neurons (common input) and the component due to an input signal independent across motor neurons. Of these signal components, the only one consistently present in all motor neuron output spike trains is that due to the input shared by all motor neurons. The other components depend on the input and on the intrinsic motor neuron properties and will be different for each motor neuron.

The above considerations indicate that by simply summing the output spike trains of several active motor neurons, to obtain what is often referred to as cumulative spike train, it is possible to enhance the output signal due to the common input and attenuate all other components. With a sufficient number of motor neurons in this averaging process, the component due to the common input will be approximately the only present in the cumulative spike train. Furthermore, in these conditions, for inputs of moderate frequency [37], the common input is transmitted undistorted by the motor neurons, so that the cumulative spike train reflects exactly the amplified common synaptic input [37], [38]. The identification of a large number of motor neurons, therefore, not only provides the neural drive sent to the muscle (motor neuron output) but also an accurate estimate of the common synaptic input that the motor neurons receive (at least for small frequency bandwidths) to generate that specific neural drive.

An alternative way to identify the characteristics of the common input to a motor neuron pool is to estimate the coherence function between the cumulative spike trains of groups of motor neurons. This analysis reveals the frequency bandwidths of the common input. Fig. 11 shows coherence functions between groups of motor units in a healthy subject and in an essential tremor patient. The coherence functions reveal different frequency characteristics of the two common inputs in the two cases, with dominant common input at the tremor frequency and its harmonics for the tremor patient.

The study of common input to a motor neuron pool has become possible thanks to the availability of methods for surface EMG decomposition that extract a large number of motor units. This analysis is of high relevance in the study of neural control of movement since the

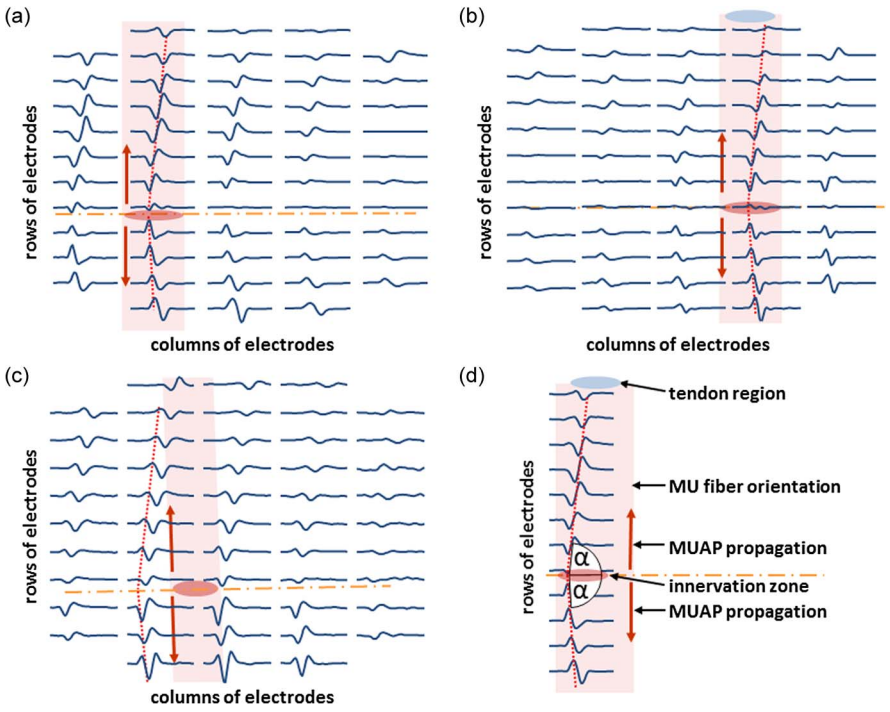

Fig. 12. *Anatomical features of motor units that can be extracted from multichannel surface MUAPs. Location and orientation of motor unit fibers are depicted by a pale red rectangle, the location of motor unit innervation zone is depicted by a red ellipse, while the tendon region is indicated by a blue ellipse. The directions of AP propagation are depicted by red arrows. The AP propagation velocity is proportional to the α angle [panel (d)]: the higher the propagation velocity the closer the α angle to 90°. Results for three motor units are depicted in panels (a), (b), and (c).*

common synaptic input to motor neurons is the only input that generates muscle force [37].

VII. FIBER ANATOMY AND MEMBRANE PROPERTIES

Once the discharge timings of a set of motor units are extracted reliably, it is possible to obtain the filters $h_{ij}(l)$ [see (1)]. These filters represent the MUAPs as detected at the recording locations. Because of the specific characteristics of the sources that represent the timings of MUAP occurrences, the filters $h_{ij}(l)$ can be obtained by spike-triggered averaging (STA) the original surface EMG signal using the discharge timings obtained from the decomposition as triggers. The averaging process enhances the MUAP (event) timed with the trigger that repeats over time and decreases the contributions of the other potentials. In this way, the signal-to-noise ratio increases as the square root of the number of triggers (for uncorrelated sources).

The multichannel single unit MUAP obtained in this fashion is the spatio–temporal electrical signature of the motor unit activation. It provides information on the muscle fiber anatomy and membrane properties. In spatial bipolar derivation, for example, it is possible, for muscles with fibers parallel to the skin plane, to identify the line where the motor unit innervation zone is distributed (Fig. 12). For bipolar recordings, this indeed corresponds to an inversion in propagation, i.e., to a change in MUAP phase in adjacent EMG channels. Moreover, if the number of electrodes is sufficient to cover the entire fiber length, the location of the tendon endings, and therefore the fiber length, can be identified. This information can be extracted either with automatic objective methods [75] or by manual segmentation of the obtained images. Fig. 12 shows examples of multichannel single MUAPs and the main anatomical features of muscle fibers that can be directly identified from these potentials.

In addition to the fiber anatomy, the multichannel MUAPs also reveal the status of the fiber membrane. This is possible by extracting the velocity of propagation (also called conduction velocity) of the potentials along the fibers [30]. Conduction velocity is determined by the status of the extracellular environment that changes with muscle activity. Therefore, it is associated to fatigue [77] and to pathological conditions [78]. Moreover, conduction velocity is proportional to fiber diameter and to the motor unit size, and therefore it can be used to distinguish motor units of different sizes and recruitment thresholds [2].

The estimation of conduction velocity from a multichannel EMG signal recorded from a muscle with fibers

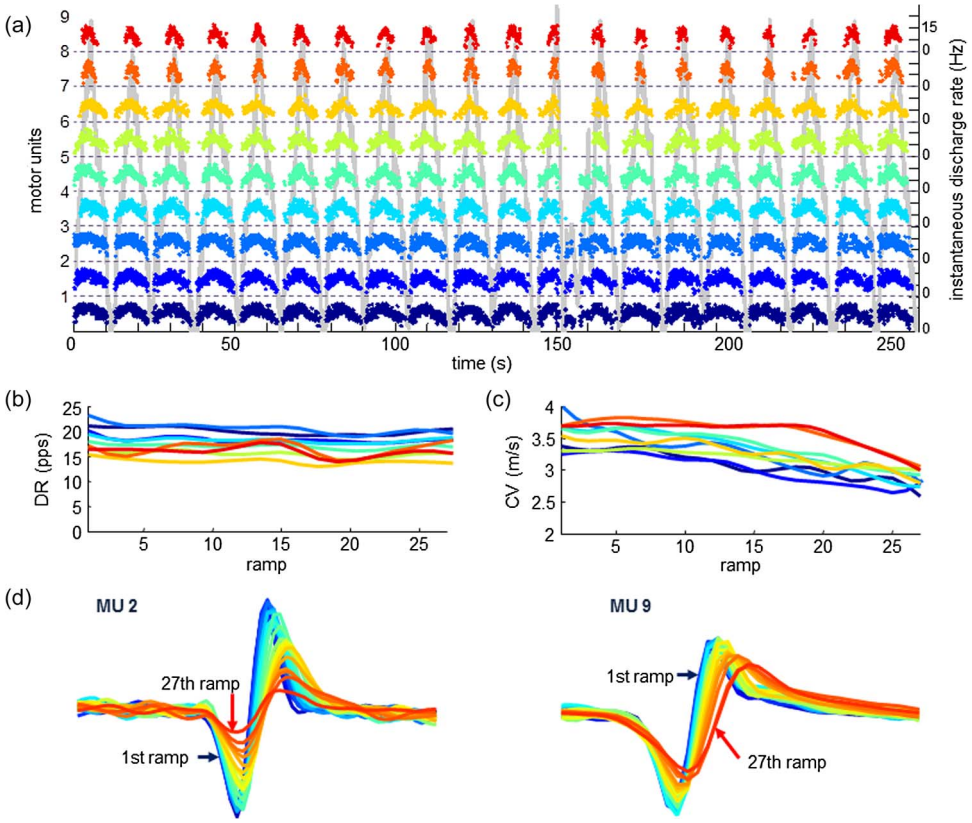

Fig. 13. *Discharge patterns of nine motor units identified by CKC decomposition from 64-channel surface EMG of the abductor pollicis brevis muscle during 27 repetitions of isometric linearly increasing and decreasing contractions (with force ranging from 0% to 10% of the maximum). In this example, ischemia was induced in the hand with a cuff around the forearm inflated at 180 mmHg in order to increase fatigue. Each dot indicates a single motor unit discharge at a given instant, whereas its relative vertical displacement codes the instantaneous motor unit discharge rate. Different motor units are depicted in different colors and are active for different proportions of time. Thus, they demonstrate different levels of fatigue. Motor units 1 to 7 gradually decrease their average conduction velocity (CV) across different contractions, whereas motor units 8 and 9 maintain the initial conduction velocity from the first to the 18th contraction, but then their conduction velocity decreases following the 18th contraction. Average motor unit discharge rates per contraction (DR) do not vary significantly over time [panel (b)]. The MUAPs of motor units 1 to 7 change significantly over the 27 contractions, while much smaller changes are observed for motor units 8 and 9. The same color in panels (a), (b), and (c) denotes the same motor unit. In panel (d), different colors denote different contractions.*

approximately parallel to the skin plane consists in the estimation of the delay between potentials detected from different recording locations along the direction of the muscle fibers. Since the conditions are nonideal and two or more potentials detected along the fiber direction are not identical, the delay is not uniquely defined and needs an optimization criterion for its identification. A classic method for the estimation of the delay between two signals is the time lag corresponding to the maximum of the cross-correlation function of the signals. This method can also be expressed in the frequency domain (spectral matching). Moreover, the extension of these approaches to more than two signals can be obtained by deriving the maximum likelihood estimator of delay, which corresponds to the minimal estimation variance in the presence of additive noise (and ideal conditions of identical shapes) [63].

In addition to the classic delay estimators briefly described above, several other approaches have been proposed [30]. Among these approaches, the use of spectral dips [31], [59] is particularly interesting since it makes use of the association between Fourier frequencies in the spatial and temporal domain for planar waves. When assuming pure propagation at constant velocity (planar wave), the signal recorded in multiple locations along the direction of propagation (z) is a spatio–temporal signal (one spatial and one temporal dimensions). For this signal, the space and time are interlinked due to the constant velocity (v), $z = vt$. As a consequence, also the Fourier frequencies in space (f_z) and time (f_t) are linked by a similar relation, $f_t = vf_z$. With many recording points, it is possible to apply a FIR spatial filter to the monopolar signal, as described above. The transfer function of this filter can be designed by assigning specific values to

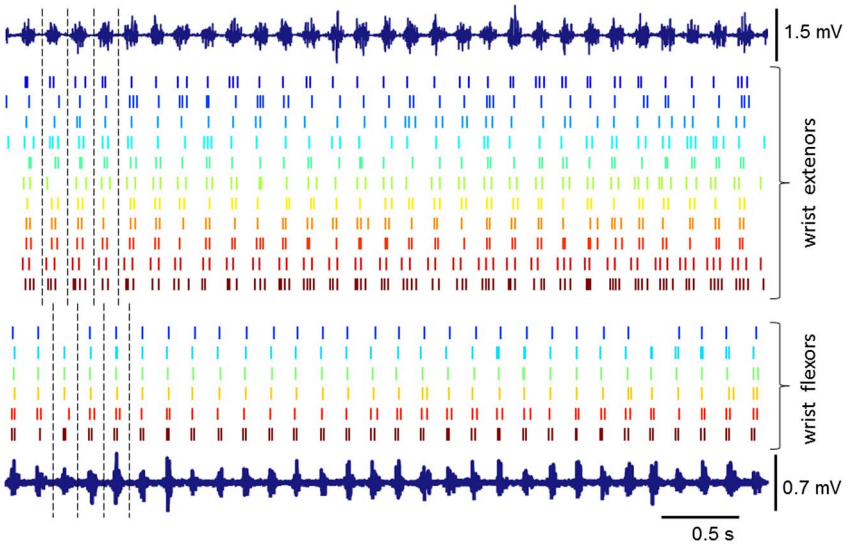

Fig. 14. *Discharge patterns of motor units of wrist extensor and flexor muscles of an essential tremor patient during an arm-outstretched task. Each vertical bar represents a discharge of individual motor unit as identified by the CKC decomposition from 64-channel surface EMG. Representative surface EMG channels are also depicted (one from the extensor—top trace—and one from flexor—bottom trace). Burst of motor unit activity are clearly visible in the surface EMG and in the motor unit discharge patterns, demonstrating high motor unit synchronization and out-of-phase tremor in the wrist extensors and flexors.*

the coefficients used to sum the signals detected at the different spatial locations. Interestingly, it is possible to impose zeros (dips) in the transfer function at specific spatial frequencies. The locations of the dips can be detected in the temporal domain from the recorded spatially filtered signal. If the location of the dips in the Fourier temporal frequency domain (f_{t0}) is detected, from the imposed location of the zeros in the spatial domain (f_{z0}) conduction velocity can be determined by the relation $f_{t0} = vf_{z0}$. With the same electrode locations, it is possible to impose dips at any frequencies (with at least four electrodes), so that the relation $f_{ti} = vf_{zi}$ is valid for infinitively many values of the imposed dips. The estimation of conduction velocity v becomes therefore a regression problem that can be solved by optimization [30].

Conduction velocity of motor units during sustained contractions is a noninvasive view into the fiber membrane properties. This measure has been used for fatigue studies [4], [64] as well as in sports sciences [66] and clinical neurophysiology [7], [78], [79]. Fig. 13 shows the changes over time of motor unit properties during a sustained contraction. The conduction velocities of all detected units decreases over time due to fatigue. In this example, also the shapes of the MUAPs vary over time, indicating that the intracellular AP shape is also varying with fatigue.

VIII. EXAMPLE OF APPLICATION: PATHOLOGICAL TREMOR

Surface EMG decomposition has recently provided the basis for the study of pathological conditions for which invasive methods for motor unit analysis are not well tolerated. A relevant example is the investigation of pathological tremor. Recently, essential tremor and Parkinsonian disease tremor have been characterized at the individual motor unit level with surface EMG decomposition [52]. Fig. 14 shows an example of such decomposition of tremoric bursts.

One of the findings obtained from the motor unit analysis of pathological tremor is that motor unit short-term synchronization is greater in pathological tremor patients than in healthy subjects. This is not due to an increase in the common synaptic input at all frequencies, but to a selective increase of the relative strength of common input specifically at the tremor frequency (Fig. 11). It has also been suggested, based on coherence between motor unit activity and EEG, that the increase in pathological common input at the tremor frequency is not exclusively due to supraspinal input but also to the spinal loop [41], [42].

The study of coherence and common input in populations of motor neurons in pathological tremor has also allowed the characterization and explanation of the phase differences between neural drives to agonist–antagonist muscles during tremor. Interestingly, agonist and antagonist muscles during tremor are not always in phase opposition but can even be activated in phase. It can indeed be shown that when the supraspinal tremor input to one muscle is weak or absent, Ia afferents provide significant common but out of phase tremor input due to passive stretch. Thus, without a voluntary drive (rest tremor) the neural drives are more likely out of

phase, while a concurrent voluntary input (postural tremor) would lead more frequently to an in-phase pattern. The experimental analysis of motor units with surface EMG decomposition has fully supported this hypothesis [42]. Indeed, coherence analysis of experimental spike trains has shown that the common tremor input is always shared by the antagonistic motoneuron pools. Moreover, it was experimentally shown that the phase difference in antogonistic motor neuron pools is different between postural and rest tremors. These results highlighted the interplay between supraspinal input and spinal afferents for tremor generation.

IX. FUTURE PERSPECTIVE

Although the processing methods described in this review allow an accurate and robust decomposition of the surface EMG in many conditions, some challenges still remain. These challenges are all related to the translation of the methods developed from the laboratory condition to the applied fields. This implies, e.g., the possibility of decomposing signals generated in dynamic conditions, with changes in joint angle and highly nonstationary conditions. Also, the decomposition should be reliable in a very broad range of conditions, including recordings with poor signal-to-noise ratio and limb anatomies with thick subcutaneous layers. The final perspective is the availability of easy to wear systems, such as those embedded in textiles, with portable wireless amplification and recording systems, and the possibility to display online during arbitrary motor tasks the activity of the motor pools of multiple muscles. This possibility would open a new window into our understanding of the neural code of movement in very general conditions.

X. CONCLUSION

In contrast to only ten years ago, today the decomposition of surface EMG into activities of individual motor units is a reality. Methods for surface EMG decomposition have been extensively validated and have been used to infer new physiological principles in the control of motor units. This has been a revolution in surface EMG processing that has led from the view of this signal as colored stochastic noise which carried information on intensity of activation mainly, to a signal comprising tens of sources discharging at precise timings that can be accurately estimated. These new view and processing methods have made possible to noninvasively decode the ultimate neural code of human movements, i.e., to describe precisely the neural drive sent to the muscle by the last neural layers of the neuromuscular system. With respect to the traditional way of estimating motor unit behavior based on invasive techniques, the surface EMG decomposition has substantially enlarged the number of sources that can be identified concurrently and the experimental conditions in which motor unit analysis can be applied. This has opened a larger window into the neural control of muscles than was available in the previous 80 years since the introduction of the concentric needle by Adrian and Bronk [1]. This new window is providing new perspectives in the principles of the neural control of muscles [81]. ■

REFERENCES

[1] E. D. Adrian and D. W. Bronk, "The discharge of impulses in motor nerve fibres," *J. Physiol.*, vol. 67, pp. 9–151, 1929.

[2] S. Andreassen and L. Arendt-Nielsen, "Muscle fibre conduction velocity in motor units of the human anterior tibial muscle: A new size principle parameter," *J. Physiol.*, vol. 391, pp. 561–571, 1987.

[3] I. Bankman, K. Johnson, and K. Schneider, "Optimal detection, classification, and superposition resolution in neural waveform recordings," *IEEE Trans. Biomed. Eng.*, vol. 40, no. 8, pp. 836–841, Aug. 1993.

[4] B. Bigland-Ritchie, E. F. Donovan, and C. S. Roussos, "Conduction velocity and EMG power spectrum changes in fatigue of sustained maximal efforts," *J. Appl. Physiol. Respir. Environ. Exerc. Physiol.*, vol. 51, no. 5, pp. 1300–1305, 1981.

[5] J. H. Blok, D. F. Stegeman, and A. van Oosterom, "Three-layer volume conductor model and software package for applications in surface electromyography," *Ann. Biomed. Eng.*, vol. 30, pp. 566–577, 2002.

[6] P. Bonato, T. D'Alessio, and M. A. Knaflitz, "Statistical method for the measurement of muscle activation intervals from surface myoelectric signal during gait," *IEEE Trans. Biomed. Eng.*, vol. 45, no. 3, pp. 287–299, Mar. 1998.

[7] O. F. Brouwer, M. J. Zwarts, T. P. Links, and A. R. Wintzen, "Muscle fiber conduction velocity in the diagnosis of sporadic hypokalemic periodic paralysis," *Clin. Neurol. Neurosurg.*, vol. 94, pp. 149–151, 1992.

[8] M. Chen and P. Zhou, "A novel framework based on FastICA for high density surface EMG decomposition," *IEEE Trans. Neural Syst. Rehabil. Eng.*, 2015, DOI: 10.1109/TNSRE.2015.2412038.

[9] R. R. L. Cisi and A. F. Kohn, "Simulation system of spinal cord motor nuclei and associated nerves and muscles, in a Web-based architecture," *J. Comput. Neurosci.*, vol. 25, pp. 520–542, 2008.

[10] E. A. Clancy and N. Hogan, "Single site electromyograph amplitude estimation," *IEEE Trans. Biomed. Eng.*, vol. 41, no. 2, pp. 159–167, Feb. 1994.

[11] E. A. Clancy and N. Hogan, "Multiple site electromyograph amplitude estimation," *IEEE Trans. Biomed. Eng.*, vol. 42, no. 2, pp. 203–211, Feb. 1995.

[12] E. A. Clancy and N. Hogan, "Probability density of the surface electromyogram and its relation to amplitude detectors," *IEEE Trans. Biomed. Eng.*, vol. 46, pp. 730–739, 1999.

[13] S. J. Day and M. Hulliger, "Experimental simulation of cat electromyogram: Evidence for algebraic summation of motor-unit action-potential trains," *J. Neurophysiol.*, vol. 86, pp. 2144–2158, 2001.

[14] C. J. De Luca, "Physiology and mathematics of myoelectric signals," *IEEE Trans. Biomed. Eng.*, pp. 313–325, 1979.

[15] C. J. De Luca, "Myoelectrical manifestations of localized muscular fatigue in humans," *Crit. Rev. Biomed. Eng.*, vol. 11, pp. 251–279, 1984.

[16] C. J. De Luca, "The use of surface electromyography in biomechanics," *J. Appl. Biomech.*, vol. 13, pp. 135–163, 1997.

[17] C. J. De Luca, A. Adam, R. Wotiz, L. D. Gilmore, and S. H. Nawab, "Decomposition of surface EMG signals," *J. Neurophysiol.*, vol. 96, pp. 1646–1657, 2006.

[18] C. J. De Luca and S. H. Nawab, "Reply to Farina and Enoka: The reconstruct-and-test approach is the most appropriate validation for surface EMG signal decomposition to date," *J. Neurophysiol.*, vol. 105, pp. 983–984, 2011.

[19] C. J. De Luca, S. H. Nawab, and J. C. Kline, "Clarification of methods used to validate surface EMG decomposition algorithms as described by Farina et al. (2014)," *J. Appl. Physiol.*, vol. 118, pp. 1084, Apr. 2015.

[20] G. V. Dimitrov and N. A. Dimitrova, "Precise and fast calculation of the motor unit potentials detected by a point and

rectangular plate electrode," *Med. Eng. Phys.*, vol. 20, pp. 374–381, 1998.

[21] G. V. Dimitrov and N. A. Dimitrova, "Fundamentals of power spectra of extracellular potentials produced by a skeletal muscle fibre of finite length. Part I: Effect of fibre anatomy," *Med. Eng. Phys.*, vol. 20, pp. 580–587, 1998.

[22] G. V. Dimitrov and N. A. Dimitrova, "Fundamentals of power spectra of extracellular potentials produced by a skeletal muscle fibre of finite length. Part II: Effect of parameters altering with functional state," *Med. Eng. Phys.*, vol. 20, pp. 702–707, 1998.

[23] N. A. Dimitrova and G. V. Dimitrov, "Interpretation of EMG changes with fatigue: Facts, pitfalls, and fallacies," *J. Electromyogr. Kinesiol.*, vol. 13, pp. 13–36, 2003.

[24] C. Disselhorst-Klug, J. Silny, and G. Rau, "Improvement of spatial resolution in surface-EMG: A theoretical and experimental comparison of different spatial filters," *IEEE Trans. Biomed. Eng.*, vol. 44, pp. 567–574, 1997.

[25] D. Farina and A. Rainoldi, "Compensation of the effect of sub-cutaneous tissue layers on surface EMG: A simulation study," *Med. Eng. Phys.*, vol. 21, pp. 487–497, 1999.

[26] D. Farina and R. Merletti, "A novel approach for precise simulation of the EMG signal detected by surface electrodes," *IEEE Trans. Biomed. Eng.*, vol. 48, pp. 637–646, 2001.

[27] D. Farina, C. Cescon, and R. Merletti, "Influence of anatomical, physical, and detection-system parameters on surface EMG," *Biol. Cybern.*, vol. 86, pp. 445–456, 2002.

[28] D. Farina, R. Merletti, and R. M. Enoka, "The extraction of neural strategies from the surface EMG," *J. Appl. Physiol.*, vol. 96, pp. 1486–1495, 2004.

[29] D. Farina, L. Mesin, S. Martina, and R. Merletti, "A surface EMG generation model with multilayer cylindrical description of the volume conductor," *IEEE Trans. Biomed. Eng.*, vol. 51, pp. 415–426, 2004.

[30] D. Farina and R. Merletti, "Methods for estimating muscle fibre conduction velocity from surface electromyographic signals," *Med. Biol. Eng. Comput.*, vol. 42, no. 4, pp. 432–445, Jul. 2004.

[31] D. Farina and F. Negro, "Estimation of muscle fiber conduction velocity with a spectral multidip approach," *IEEE Trans. Biomed. Eng.*, vol. 54, pp. 1583–1589, 2007.

[32] D. Farina, "Counterpoint: Spectral properties of the surface EMG do not provide information about motor unit recruitment and muscle fiber type," *J. Appl. Physiol.*, vol. 105, pp. 1673–1674, 2008.

[33] D. Farina, F. Negro, M. Gazzoni, and R. M. Enoka, "Detecting the unique representation of motor-unit action potentials in the surface electromyogram," *J. Neurophysiol.*, vol. 100, pp. 1223–1233, 2008.

[34] D. Farina, C. Cescon, F. Negro, and R. M. Enoka, "Amplitude cancellation of motor-unit action potentials in the surface electromyogram can be estimated with spike-triggered averaging," *J. Neurophysiol.*, vol. 100, pp. 431–440, 2008c.

[35] D. Farina and R. M. Enoka, "Surface EMG decomposition requires an appropriate validation," *J. Neurophysiol.*, vol. 105, pp. 981–982, 2011.

[36] D. Farina, R. Merletti, and R. M. Enoka, "The extraction of neural strategies from the surface EMG: An update," *J. Appl. Physiol.*, vol. 117, pp. 1215–1230, 2014.

[37] D. Farina, F. Negro, and J. L. Dideriksen, "The effective neural drive to muscles is the common synaptic input to motor neurons," *J. Physiol.*, vol. 592, pp. 3427–3441, 2014.

[38] D. Farina and F. Negro, "Common synaptic input to motor neurons, motor unit synchronization, and force control," *Exerc. Sport Sci. Rev.*, vol. 43, pp. 23–33, 2015.

[39] D. Farina, R. Merletti, and R. M. Enoka, "Reply to De Luca, Nawab, and Kline: The proposed method to validate surface EMG signal decomposition remains problematic," *J. Appl. Physiol.*, vol. 118, pp. 1085, 2015.

[40] D. A. Gabriel, S. M. Lester, S. A. Lenhardt, and E. D. Cambridge, "Analysis of surface EMG spike shape across different levels of isometric force," *J. Neurosci. Methods*, vol. 159, pp. 146–152, 2007.

[41] J. A. Gallego *et al.*, "Influence of common synaptic input to motor neurons on the neural drive to muscle in essential tremor," *J. Neurophysiol.*, vol. 113, pp. 182–191, 2015.

[42] J. A. Gallego *et al.*, "The phase difference between neural drives to antagonist muscles in essential tremor is associated to the relative strength of supraspinal and afferent input," *J. Neurosci.*, vol. 35, no. 23, pp. 8925–8937, 2015.

[43] V. Glaser, A. Holobar, and D. Zazula, "Real-time motor unit identification from high-density surface EMG," *IEEE Trans. Neural Syst. Rehabil. Eng.*, vol. 21, pp. 949–958, 2013.

[44] T. H. Gootzen, D. F. Stegeman, and A. Van Oosterom, "Finite limb dimensions and finite muscle length in a model for the generation of electromyographic signals," *Electroencephalogr. Clin. Neurophysiol.*, vol. 81, pp. 152–162, 1991.

[45] A. Holobar, C. Fevotte, C. Doncarli, and D. Zazula, "Single autoterms selection for blind source separation in time-frequency plane," in *Proc. EUSIPCO*, 2002, pp. 565–568.

[46] A. Holobar and D. Zazula, "Surface EMG decomposition using a novel approach for blind source separation," *Informatica Medica Slovenica*, vol. 8, pp. 2–14, 2003.

[47] A. Holobar and D. Zazula, "Correlation-based decomposition of surface electromyograms at low contraction forces," *Med. Biol. Eng. Comput.*, vol. 42, pp. 487–495, 2004.

[48] A. Holobar and D. Zazula, "Multichannel blind source separation using convolution kernel compensation," *IEEE Trans. Signal Process.*, vol. 55, pp. 4487–4496, 2007.

[49] A. Holobar and D. Zazula, "Gradient convolution kernel compensation applied to surface electromyograms," in *Independent Component Analysis and Signal Separation* Lecture Notes in Computer Science. Berlin, Germany: Springer-Verlag, 2007, vol. 4666, pp. 617–624.

[50] A. Holobar, D. Farina, M. Gazzoni, R. Merletti, and D. Zazula, "Estimating motor unit discharge patterns from high-density surface electromyogram," *Clin. Neurophysiol.*, vol. 120, pp. 551–562, 2009.

[51] A. Holobar, M. A. Minetto, A. Botter, F. Negro, and D. Farina, "Experimental analysis of accuracy in the identification of motor unit spike trains from high-density surface EMG," *IEEE Trans. Neural Syst. Rehabil. Eng.*, vol. 18, pp. 221–229, 2010.

[52] A. Holobar, V. Glaser, J. A. Gallego, J. L. Dideriksen, and D. Farina, "Non-invasive characterization of motor unit behaviour in pathological tremor," *J. Neural Eng.*, vol. 9, 2012, Art. ID 056011.

[53] A. Holobar, M. A. Minetto, and D. Farina, "Accurate identification of motor unit discharge patterns from high-density surface EMG and validation with a novel signal-based performance metric," *J. Neural Eng.*, vol. 11, 2014, Art. ID 016008.

[54] X. Hu, W. Z. Rymer, and N. L. Suresh, "Assessment of validity of a high-yield surface electromyogram decomposition," *J. Neuroeng. Rehabil.*, vol. 10, pp. 99, 2013.

[55] A. Hyvärinen and E. Oja, "A fast fixed-point algorithm for independent component analysis," *Neural Comput.*, vol. 9, pp. 1483–1492, 1997.

[56] A. Hyvärinen and E. Oja, "Independent component analysis: Algorithms and applications," *Neural Netw.*, vol. 13, pp. 411–430, 2000.

[57] K. G. Keenan, D. Farina, K. S. Maluf, R. Merletti, and R. M. Enoka, "Influence of amplitude cancellation on the simulated surface electromyogram," *J. Appl. Physiol.*, vol. 98, pp. 120–131, 2005.

[58] K. G. Keenan, D. Farina, R. Merletti, and R. M. Enoka, "Amplitude cancellation reduces the size of motor unit potentials averaged from the surface EMG," *J. Appl. Physiol.*, vol. 100, pp. 1928–1937, 2006.

[59] L. H. Lindstrom and R. I. Magnusson, "Interpretation of myoelectric power spectra: A model and its applications," *Proc. IEEE*, vol. 65, no. 5, pp. 653–662, May 1977.

[60] M. M. Lowery, N. S. Stoykov, A. Taflove, and T. A. Kuiken, "A multiple-layer finite-element model of the surface EMG signal," *IEEE Trans. Biomed. Eng.*, vol. 49, pp. 446–454, 2002.

[61] B. Mambrito and C. J. De Luca, "A technique for the detection, decomposition and analysis of the EMG signal," *Electroencephalogr. Clin. Neurophysiol.*, vol. 58, pp. 175–188, 1984.

[62] T. Masuda, H. Miyano, and T. Sadoyama, "A surface electrode array for detecting action potential trains of single motor units," *Electroencephalogr. Clin. Neurophysiol.*, vol. 60, pp. 435–443, 1985.

[63] K. C. McGill and L. J. Dorfman, "High-resolution alignment of sampled waveforms," *IEEE Trans. Biomed. Eng.*, vol. 31, pp. 462–468, 1984.

[64] R. Merletti, M. Knaflitz, and C. J. De Luca, "Myoelectric manifestations of fatigue in voluntary and electrically elicited contractions," *J. Appl. Physiol.*, vol. 69, pp. 1810–1820, 1990.

[65] R. Merletti and L. R. Lo Conte, "Advances in processing of surface myoelectric signals: Part 1," *Med. Biol. Eng. Comput.*, vol. 33, pp. 362–372, 1995.

[66] M. A. Minetto *et al.*, "Interleukin-6 response to isokinetic exercise in elite athletes: Relationships to adrenocortical function and to mechanical and myoelectric fatigue," *Eur. J. Appl. Physiol.*, vol. 98, pp. 373–382, 2006.

[67] S. H. Nawab, S. S. Chang, and C. J. De Luca, "High-yield decomposition of surface EMG signals," *Clin. Neurophysiol.*, vol. 121, pp. 1602–1615, 2010.

[68] F. Negro and D. Farina, "Linear transmission of cortical oscillations to the neural drive to muscles is mediated by common projections to populations of motoneurons

in humans," *J. Physiol.*, vol. 589, pp. 629–637, 2011.

[69] V. T. Ramaekers *et al.*, "Clinical application of a noninvasive multi-electrode array EMG for the recording of single motor unit activity," *Neuropediatrics*, vol. 24, pp. 134–138, 1993.

[70] G. Rau, C. Disselhorst-Klug, and J. Silny, "Noninvasive approach to motor unit characterization: Muscle structure, membrane dynamics and neuronal control," *J. Biomech.*, vol. 30, pp. 441–446, 1997.

[71] P. Ravier, O. Buttelli, R. Jennane, and P. Couratier, "An EMG fractal indicator having different sensitivities to changes in force and muscle fatigue during voluntary static muscle contractions," *J. Electromyogr. Kinesiol.*, vol. 15, pp. 210–221, 2005.

[72] H. Reucher, G. Rau, and J. Silny, "Spatial filtering of noninvasive multielectrode EMG: Part I—Introduction to measuring technique and applications," *IEEE Trans. Biomed. Eng.*, vol. 34, pp. 98–105, 1987.

[73] H. Reucher, J. Silny, and G. Rau, "Spatial filtering of noninvasive multielectrode EMG: Part II—Filter performance in theory and modelling," *IEEE Trans. Biomed. Eng.*, vol. 34, pp. 106–113, 1987.

[74] D. Stashuk, "EMG signal decomposition: How can it be accomplished and used?" *J. Electromyogr. Kinesiol.*, vol. 11, no. 3, pp. 151–173, Jun. 2001.

[75] K. Ullah, C. Cescon, B. Afsharipour, and R. Merletti, "Automatic detection of motor unit innervation zones of the external anal sphincter by multichannel surface EMG," *J. Electromyogr. Kinesiol.*, vol. 24, pp. 860–867, 2014.

[76] V. von Tscharner and B. M. Nigg, "Point: Spectral properties of the surface EMG can characterize/do not provide information about motor unit recruitment strategies and muscle fiber type," *J. Appl. Physiol.*, vol. 105, pp. 1671–1673, 2008.

[77] M. J. Zwarts, T. W. Van Weerden, and vH. T. Haenen, "Relationship between vaverage muscle fibre conduction velocity and EMG power spectra during isometric contraction, recovery and applied ischemia," *Eur. J. Appl. Physiol. Occup. Physiol.*, vol. 56, pp. 212–216, 1987.

[78] M. J. Zwarts, T. W. van Weerden, T. P. Links, H. T. Haenen, and H. J. Oosterhuis, "The muscle fiber conduction velocity and power spectra in familial hypokalemic periodic paralysis," *Muscle Nerve*, vol. 11, pp. 166–173, 1988.

[79] J. H. Van der Hoeven, M. J. Zwarts, and T. W. Van Weerden, "Muscle fiber conduction velocity in amyotrophic lateral sclerosis and traumatic lesions of the plexus brachialis," *Electroencephalogr. Clin. Neurophysiol.*, vol. 89, pp. 304–310, 1993.

[80] F. Negro, S. Muceli, M. Castronovo, A. Holobar, and D. Farina, "Multi-channel intramuscular and surface EMG decomposition by convolutive blind source separation", 2015.

[81] D. Farina, F. Negro, S. Muceli, and R. Enoka, "Principles of motor unit physiology evolve with advances in technology," *Physiology*, 2015.

ABOUT THE AUTHORS

Dario Farina (Senior Member, IEEE) received the M.Sc. degree in electronics engineering from Politecnico di Torino, Torino, Italy, in 1998, the Ph.D. degree in automatic control and computer science from the Ecole Centrale de Nantes, Nantes, France, in 2001, and the Ph.D. degree in electronics and communications engineering from Politecnico di Torino in 2002.

From 1997 to 2004, he was a Researcher at the Laboratory for Neuromuscular System Engineering (LISiN), Politecnico di Torino. During 2004–2008, he was an Associate Professor in Biomedical Engineering at Aalborg University, Aalborg, Denmark. At the same university, in 2008, he became Full Professor in Motor Control and Biomedical Signal Processing and the Head of the Research Group on Neural Engineering and Neurophysiology of Movement. In 2010, he was appointed Full Professor and Founding Chair of the Department of Neurorehabilitation Engineering at the University Medical Center Göttingen, Georg-August University, Göttingen, Germany, within the Bernstein Focus Neurotechnology (BFNT) Göttingen. In this position, he has also been the Chair for NeuroInformatics of the BFNT Göttingen since 2010. His research focuses on neurorehabilitation technology, neural control of movement, and biomedical signal processing and modeling. Within these areas, Prof. Farina has (co)authored more than 350 papers in peer-reviewed journals and over 400 among conference papers/abstracts, book chapters, and encyclopedia contributions.

Prof. Farina was the President of the International Society of Electrophysiology and Kinesiology (ISEK) in 2012–2014 and currently holds the position of Past President. Among other awards, he has been the recipient of the 2010 IEEE Engineering in Medicine and Biology Society Early Career Achievement Award for his contributions to biomedical signal processing and to electrophysiology; in 2012, he was elected Fellow of the American Institute for Medical and Biological Engineering (AIMBE); and is currently a Distinguished Lecturer of the IEEE. He is the Editor-in-Chief of the *Journal of Electromyography and Kinesiology*, and an Associate Editor of the IEEE TRANSACTIONS ON BIOMEDICAL ENGINEERING, Medical & Biological Engineering & Computing, and *The Journal of Physiology*.

Aleš Holobar (Member, IEEE) received the Ph.D. degree in computer science from the Faculty of Electrical Engineering and Computer Science (FEECS), University of Maribor, Maribor, Slovenia, in 2004.

From 2005 to 2008, he held postdoctoral appointments at the Laboratory of Engineering of Neuromuscular System and Motor Rehabilitation at Politechnico di Torino, Torino, Italy. Since 2009, he has held the position of an Associate Professor at FEECS. His main research interests include statistical signal processing, compound signal decomposition, identification of multidimensional systems and biomedical imaging with current activities focused on surface electromyography, electroencephalography, and biomedical signal processing. He has (co)authored two book chapters, 45 papers in peer-reviewed journals, over 70 conference contributions, and one patent.

Dr. Holobar is a member of the International Society of Electrophysiology and Kinesiology (ISEK), International Association of Pattern Recognition (IAPR), the Slovenian Association of Technical and Natural Sciences (SATENA), and the Slovenian Society of Pattern Recognition.